POLITECNICO DI TORINO

Department of Mechanical and Aerospace Engineering
Master's Degree in Automotive Engineering

Master's Degree Thesis

Experimental Analysis on Electric–Kick Scooter

Supervisor

Prof. Alessandro Vigliani
Ing. Angelo Domenico Vella

Candidate

Aadharsh Yazhisaivendhan

Experimental Analysis on Electric–Kick Scooter

Aadharsh Yazhisaivendhan [1]
[1] Politecnico di Torino, Department of Mechanical and Aerospace Engineering
Corso Duca degli Abruzzi, 24 – 10129, Torino, Italy

Acknowledgement

First and foremost, I wish to express my sincere gratitude to Professor Alessandro Vigliani for his expert advice and for providing me an opportunity to work with him. A true belief helped me gain the experience of working on such an amazing project. His constant support and honest attitude were exemplary, and exactly what was needed to get the task done.

I sincerely would like to thank Angelo Domenico Vella for his guidance and encouragement in carrying out this project work. Also, the advisory help I received in achieving the set goals to complete the project was a real piece of admiration. The faith and support were invaluable.

Lastly, I would like to thank my family and friends, who gave me the strength and power to face all the challenges both in the conduct of the thesis and in life. They have provided me with unconditional support and encouragement throughout all these years.

INDEX

LIST OF FIGURES

LIST OF TABLES

Abstract

Due to the novelty of the topic and the rapid expansion of e-scooter systems, it has led to an increasing number of injuries. A large proportion of injuries are related to the vehicles themselves. Therefore, a thorough investigation of their safety is required. The purpose of the thesis is to collect substantiation for or against the safety level of e-scooters, in terms of rider safety and comfort. MI Pro 2 was used to record the kinematic data recorded using sensors mounted on the e-scooter. A set of performance indicators were studied to be able to compare the e-scooter and establish its safety.

This thesis aims at providing data through experimental analysis and comparing them with different sets of constraints. The tests were mainly focused on the longitudinal and vertical dynamics of the e-scooter as they contribute to the rider's comfort and safety. The tests include coastdown testing to compute the resistance forces acting on the e-scooter by presenting the range of vibrations acting in different positions within the e-scooter. The accelerations were also computed followed by signal processing using MATLAB software.

Results suggest that the e-scooter performed very well in terms of rider comfort and safety. It also had good maneuverability with decent braking performances. Future studies could include experiments in more naturalistic settings that could provide valuable data to extend the results presented in this thesis. The results from this thesis could be used to help improve the design of electric scooters and contribute to the guidelines for infrastructure design and policy making.

1. Introduction

The development of electric scooter is inspired from the concept of motorized scooters which dates as far back as the early 1800s. Over the next century, the Autoped was designed which was quite similar to the modern electric scooter, but it was bulkier due to the technology restrictions and the machine was gas-powered. The objective of the invention was to produce a vehicle which would be extremely small, compact, and light in comparison to the load to be carried and will be sufficiently powerful to offer adequate means for quick locomotion under ordinary conditions and relatively extreme economy in use and operation. The electric scooters become popular not until 2018, when the GPS-powered dockless bike rental services started throughout big cities.

In this thesis, the research focuses on the safety and dynamics of the electric scooter. More clearly, the main objective is to estimate the forces acting on the e-scooter and study them in order to understand its general behaviour which in turn concerns the safety of the passenger. The tests were performed considering various parameters such as, tire pressure, weather conditions (when a particular test was performed), and the asphalt condition.

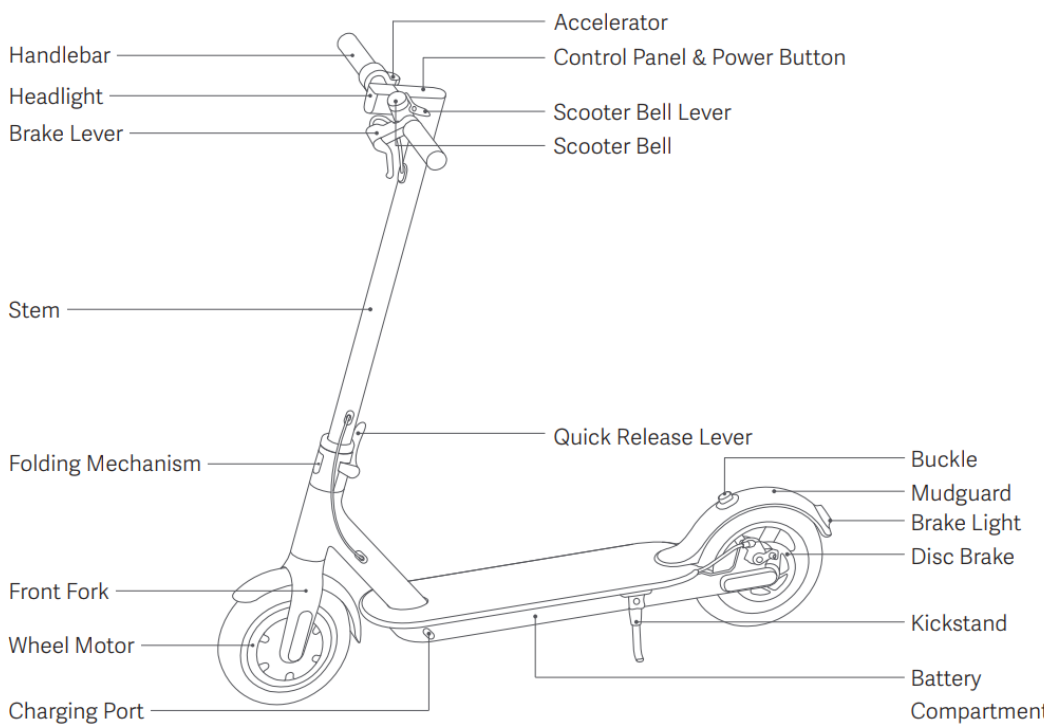

Figure 1.1 – MI Electric Scooter Pro II (Test specimen)

Figure 1.1 shows the overview of the test specimen. The control panel has a power button to switch on/off the scooter and the speedometer present in the control panel displays the current speed of the scooter, and also, it displays the error codes. There are three riding modes available:

- ECO – for energy saving mode (top speed approximately 15 km/h, smooth throttle).
- D – for standard mode (top speed approximately 20 km/h).
- S – for sport mode (top speed approximately 25 km/h, powerful).
  The control panel has an icon to display the bluetooth connectivity with a mobile device. It also has a battery power indicator (indicated by 5 bars, each representing approximately 20% of a full battery).

Figure 1.2 – Dimensions: Folded (left) and Unfolded (right)

Table 1.1 – Technical Specification of the e-scooter

	Unit	**Value**
Name	-	Mi Electric Scooter Pro
Model	-	DDHBC02NEB
Dimensions	cm	113 x 43 x 118 (unfolded) 113 x 43 x 49 (folded)
Net Weight	kg	14.2
Load Range	kg	100
Max. Speed	km/h	~ 25
Range	km	~ 45
Max. Climbing Angle	%	~ 20
Charging Time	h	~ 8
Rated Voltage	V	37
Max. Input Voltage	V	42
Rated Capacity	Wh	474
Rated Power	kW	0.3
Max. Power	kW	0.6

1.1 Inertial parameter identification

The information of the inertia parameters, namely, mass, the location of centre of gravity and inertia tensor which includes the moments and products of inertia of a mechanical system is of utmost importance during the study of dynamic behaviour of a body. This is solely applicable when the motion of a rigid body is to be examined or characterized.

1.1.1 Weighing method

The mass can be characterized by the standard weighing method using weighing scales. The weight of the specimen is determined and subsequently converted to mass.

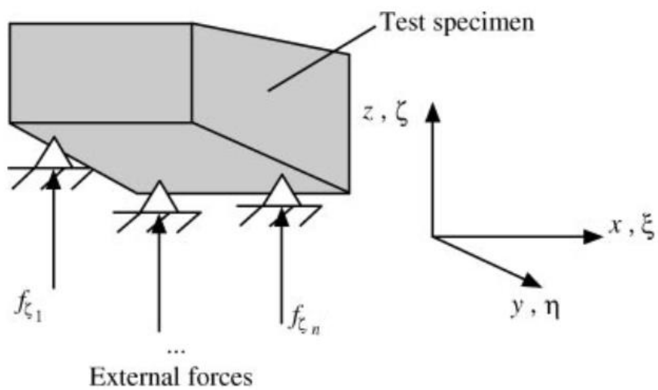

Figure 1.1.1.1 – Principle of weighing method

The external forces are measured, and the mass is directly derived from the equation below.

$$m = \frac{\sum_i f_{\zeta_i}}{g}$$

The e-scooter was placed over a weighing machine whose weight was observed to be **14.2 kg.** Using the above formula, the mass of the e-scooter can be calculated.

$$m = \frac{14.2}{9.81} = 1.448\ kg$$

1.1.2 Suspension Method

The inertial parameters can be identified using widely accepted industrial method called static ***suspension method.*** The suspension method yields the centre of gravity location of the test specimen. The test specimen is consecutively suspended at several points, e.g. by using a wire. The intersection point of all wire lines represents the location of centre of gravity (Figure 2.1.2.1). At least two suspension points are necessary in order to locate the centre of gravity location.

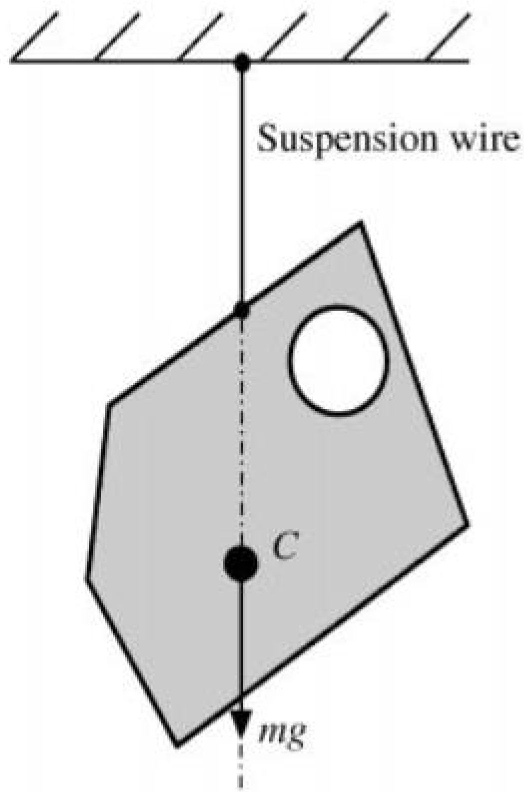

Figure 1.1.2.1 – Principle of suspension method

The suspension method is commonly applied and approved in industry. In this method, the selection of wire is important, and the need of software is not necessary. The only disadvantage being the time required to numerically determine the coordinates of the centre of gravity.

Barycenter Analysis

The barycenter of the e-scooter was analysed using the method mentioned above. Suspension chains were used to mount at two different configurations for approximately locating the intersecting point. The setup is shown in Figure 1.1.2.2.

The inclination of axes was measured using a mobile application with a tolerance of $\pm 1°$. The intersection point may vary depending on the suspension wire which implies the accuracy of the method to be low. This method only gives an approximate location of the actual barycenter. The inclination was noted as shown in Figure 1.1.2.3. Also, a schematic of the analysis of the barycenter location is shown in Figure 1.1.2.5.

Figure 1.1.2.2 – Configuration 1 (left) and configuration 2 (right)

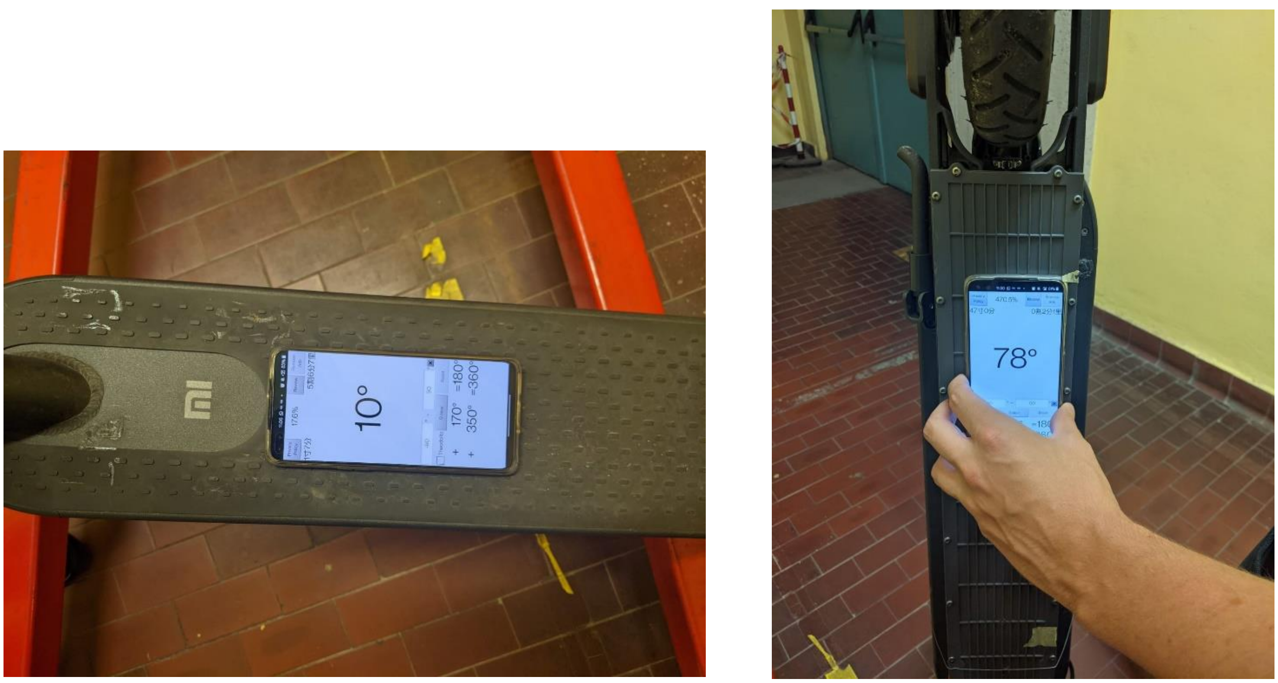

Figure 1.1.2.3 – Inclination of the e-scooter for configuration 1 (left) and for configuration 2 (right)

The estimate was made by drafting a free body diagram using Autodesk AutoCAD. The FBD of the test specimen is presented in Figure 1.1.1.4.

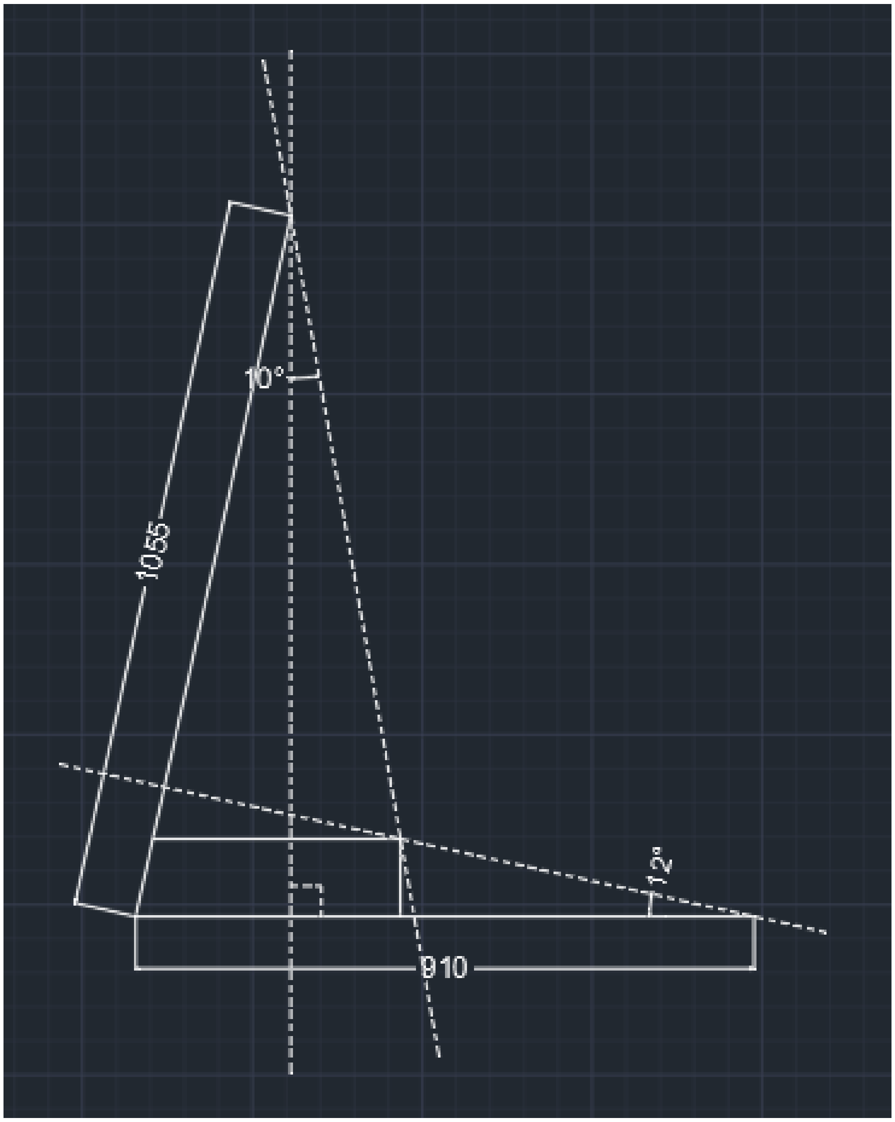

Figure 1.1.2.4 – FBD of the test specimen

Table 1.1.1.1 – Co-ordinates of the centre of gravity

Reference Point	Nomenclature	Distance [mm]
COG to front wheel centre	AC	334
COG to rear wheel centre	BC	528
COG to ground	DE	233

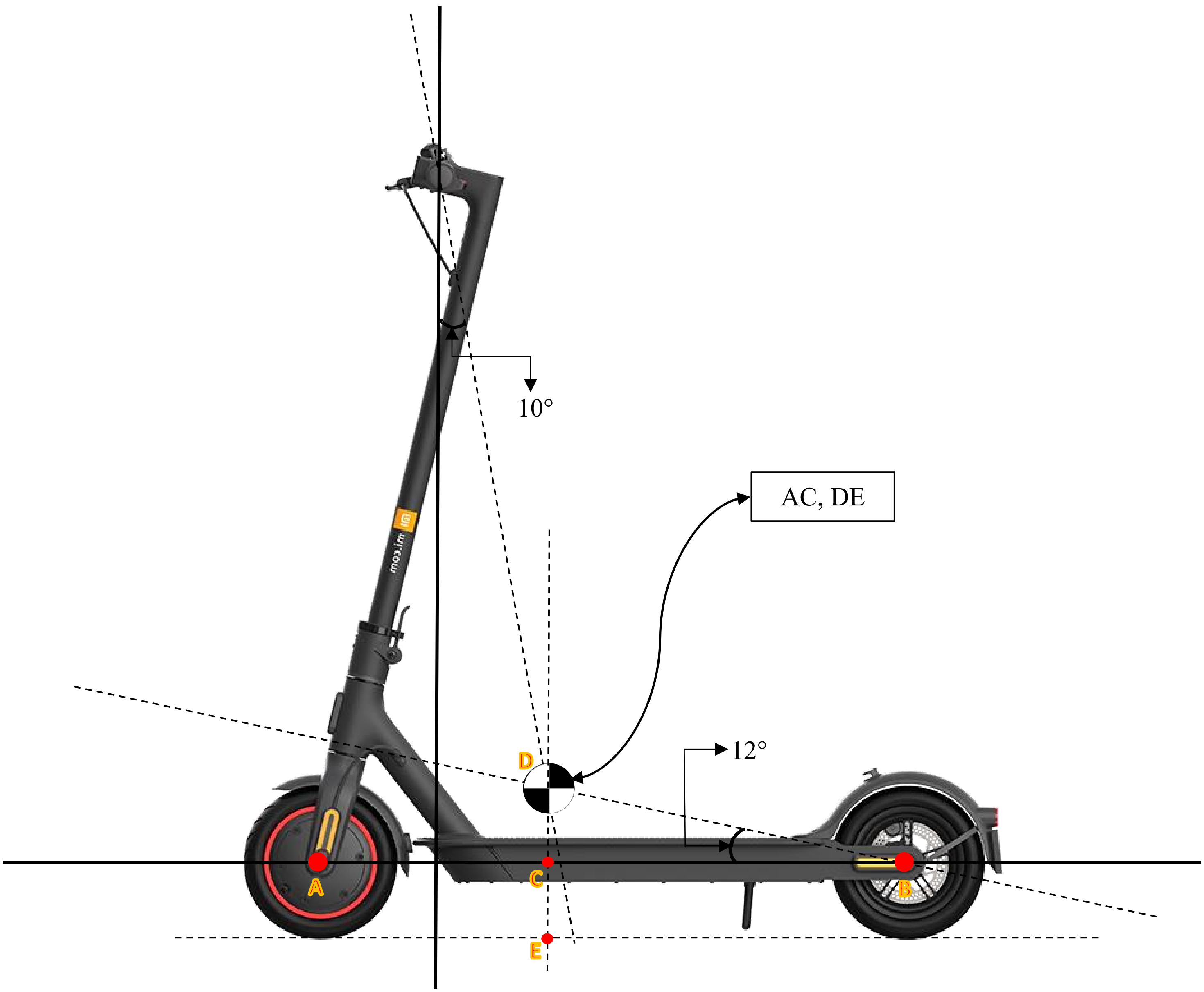

Figure 1.1.2.5 – Barycenter co-ordinates

The co-ordinates for the location of barycenter, as shown in Figure 1.1.1.5 is an approximate value of the actual barycenter. Furthermore, the nomenclature and reference points of the co-ordinates of the barycenter are tabulated in Table 1.1.1.1.

1.1.3 Gravitational Pendulum Method

Another significant and helpful method which is used to determine the inertial parameters is based on small angular motions. It is called ***gravitational pendulum method***. The moment of inertia about a specified pendulum axis can be estimated by supporting the test specimen by knife edges or suspending by wires (Figure 1.1.3.1).

The test specimen acts as a physical pendulum while the restoring torque is generated by gravitation. If the mass and the centre of gravity of the specimen is known, the moment of inertia about the pendulum axis can be evaluated from the measured oscillation frequency (absolute method). Otherwise, if only the mass of the specimen is known, the moment of inertia about the pendulum axis can be evaluated using the measured oscillation frequencies of two tests with different wire lengths (relative method).

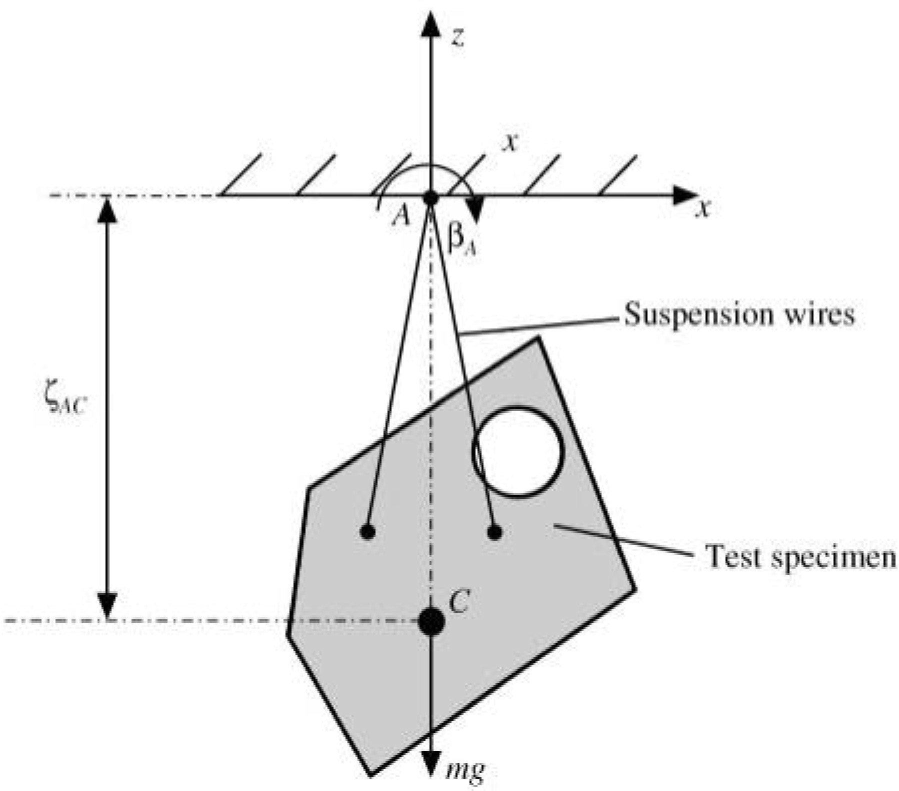

Figure 1.1.3.1 – Principle of gravitational pendulum method

The mechanical system is mounted such that pendulum axis and y-axis of the inertial frame coincide. The η-axis of the body fixed frame is chosen to be co-linear to the y-axis of the inertial frame (Figure 2.1.3.1). Thus, if no external torques act, the simplified equation is given as:

$$\theta_{A\eta\eta}\ddot{\beta}_A + mg\zeta_{AC}\beta_A = 0$$

This is the equation of motion of a single-degree-of-freedom oscillator. If the mass and the location of centre of gravity are known, the moment of inertia can be directly estimated using the measured frequency oscillation frequency, f_0:

$$\theta_{A\eta\eta} = \frac{mg\zeta_{AC}}{(2\pi f_0)^2}$$

In order to complete the inertia tensor, at least six tests with different specified pendulum axes are required. It is necessary that the pendulum axes intersect at one single point.
The gravitational pendulum method is approved in industry and the only hardware required is a suspension wire. The limitations of this method being the time required for testing and data processing are high because only one moment of inertia can be estimated simultaneously.

Estimation of moment of inertia

The gravitational pendulum method is a better and easier method to evaluate the moment of inertia of an e-scooter. The description of the technique is explained thoroughly as discussed above. The only challenge is to be able to mount the hinge and the sensor.

Figure 1.1.3.2 shows the mounting of the sensor on the e-scooter and, the hinge and the suspension chain mounted on the pulley.

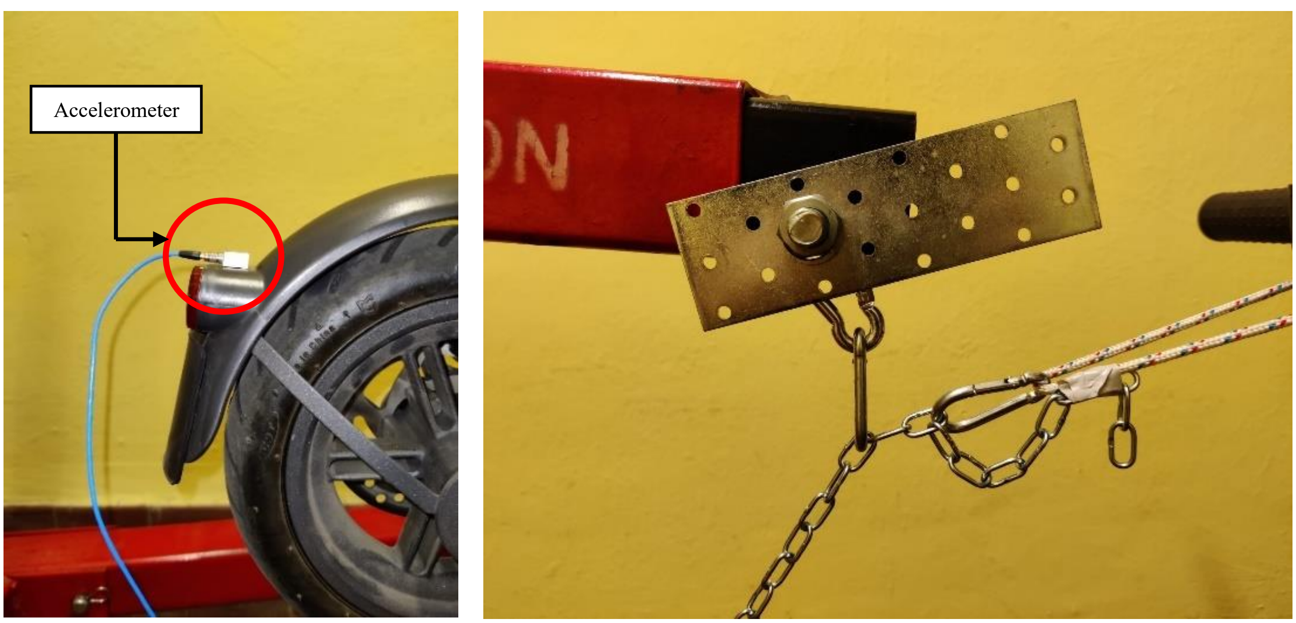

Figure 1.1.3.2 – Accelerometer (left) and hinge point (right)

The closer the hinge is to the barycenter, the more accurate are the results. The front part of the e-scooter was locked using cable ties and tape to restrict the motion of steering rod as shown in Figure 1.1.3.3.

Figure 1.1.3.3 – Locking of steering rod

Figure 1.1.3.4 – Experimental setup; top view (left) and side view (right)

Using the parallel axis theorem, and relative gravitational pendulum method, where in the difference in change in the length of the suspension wire is utilized, the estimate of the moment of inertia of the test specimen in the desired axis is calculated analytically.

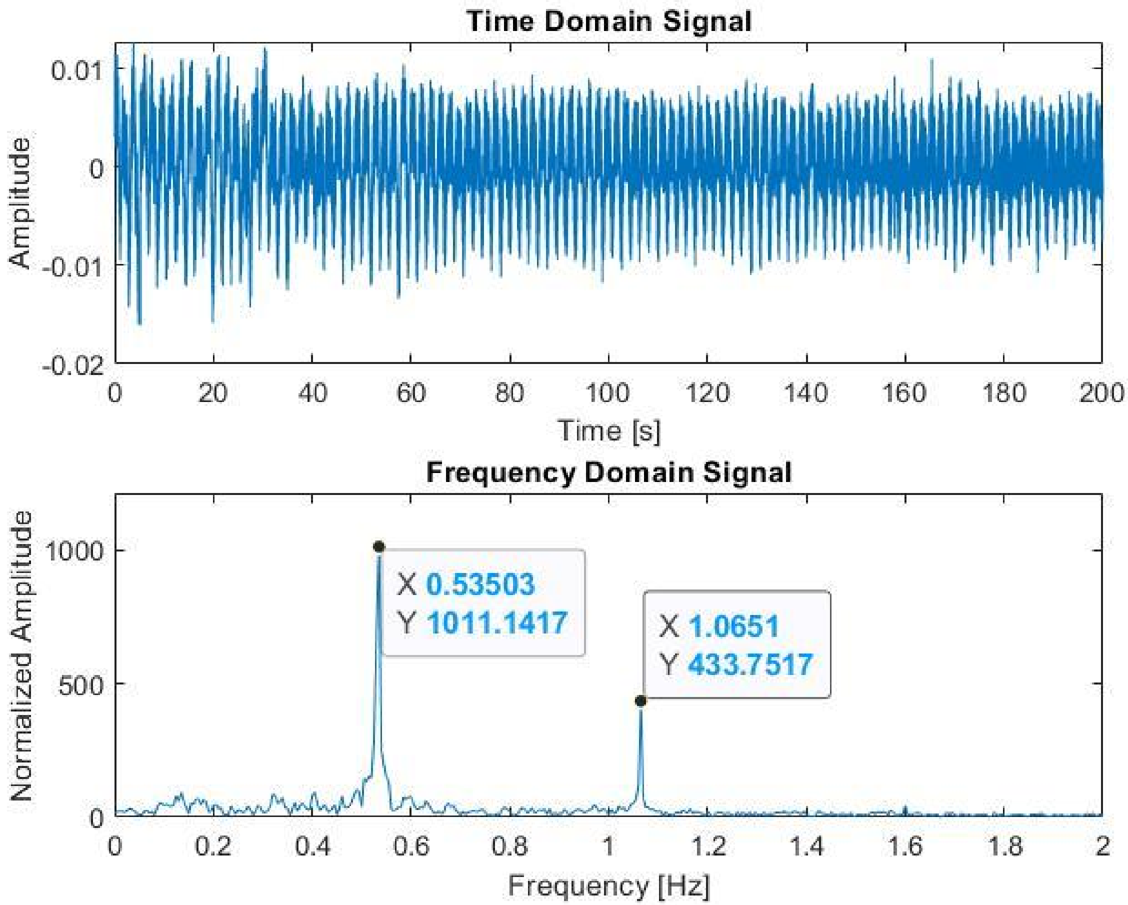

Figure 1.1.3.5 – Frequency analysis (x-direction)

Table 1.1.3.1 – Frequency analysis (x-direction)

Configuration	**Test Number**	**Frequency [Hz]**		**Average Frequency [Hz]**	
		Low	**High**	**Low**	**High**
1	1	0.53503	1.0651	0.54	1.10
	2	0.53503	1.0651		
	3	0.53503	1.0651		
2	1	0.48503	0.97005	0.49	1.00
	2	0.48503	0.97005		
	3	0.48503	0.97005		

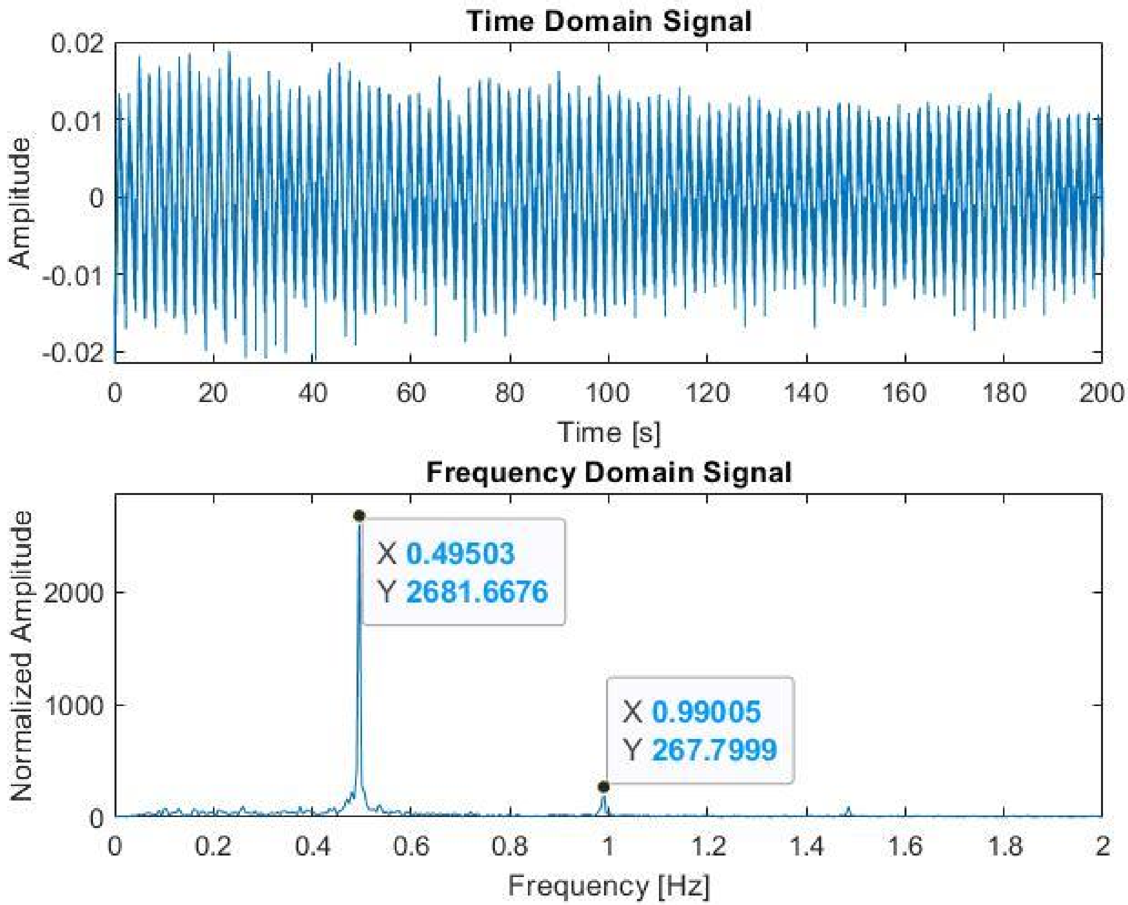

Figure 1.1.3.6 – Frequency analysis (y-direction)

Table 1.1.3.2 – Frequency analysis (y-direction)

Configuration	**Test Number**	**Frequency [Hz]**		**Average Frequency [Hz]**	
		Low	**High**	**Low**	**High**
1	1	0.49503	0.98505	0.50	1.00
	2	0.49503	0.99005		
	3	0.49503	0.99005		
2	1	0.46502	1.3901	0.47	1.40
	2	0.46502	1.3901		
	3	0.46002	1.3851		

The first frequency (low) is dependent on the 1st order of the equation and the second frequency (high) is dependent on the 2nd order of the equation for a generic point in the body. Due to very small angular acceleration, the second order term can be neglected.

Thus the equation gets reduced to:

$$J_{zo} = \frac{mgL}{(2\pi f_z)^2}$$

Using the parallel axis theorem, the moment of inertia of the e-scooter can be calculated as:

$$J_{zg} = J_{zo} - ml^2$$

where,
J_{zo} = moment of inertia about point O
J_{zg} = moment of inertia of the e-scooter about centre of gravity
L = length of the axis from the barycenter
l = distance between the axes about the barycenter and point O

As discussed previously, the gravitational pendulum method (relative) method was used where the difference in the wire length was noted to be 200 mm, i.e., $\Delta L = 200\ mm$. The moment of inertia of the e-scooter about the axis of centre of gravity was calculated analytically and tabulated in Table 1.1.3.3.

Table 1.1.3.3 – Moment of inertia about centre of gravity

Position of centre of gravity	(334,233) mm
Weight (W)	14.2 kg
Inertia about x-axis (J_{xx})	1602.721 kg-mm^2
Inertia about y-axis (J_{yy})	1835.032 kg-mm^2

The position of centre of gravity in Table 1.1.3.3 is mentioned with reference to Figure 1.1.2.5.

2. Methodology

The thesis is based primarily on the safety of the passenger driving the e-scooter. The characteristics of the e-scooter is analyzed thoroughly, by performing various tests with different parameters using sensors mounted on the scooter.

The dynamics of a ground vehicle is characterized by their longitudinal, lateral, and vertical motions. The first part of the thesis is based on the longitudinal dynamics of the e-scooter which is an important aspect of the safety of the passengers. The information was gathered in real time with the setup including sensors and the acquisition system shown in the figure.

2.1 The System

The e-scooter was equipped with sensors to collect real-time data. The sensors mounted on the scooter are described below.

IMU: An inertial measurement unit used for evaluation the forces acting on the e-scooter.
GPS: Used to track the distance and velocity of the e-scooter.
Proximity Sensor: Used to track voltage pulse for velocity tracking.
Siemens SCADAS XS: An acquisition system which stores the information from various tests performed.

The mounting location of each sensor and the acquisition system is shown in the Figure 2.1.1.

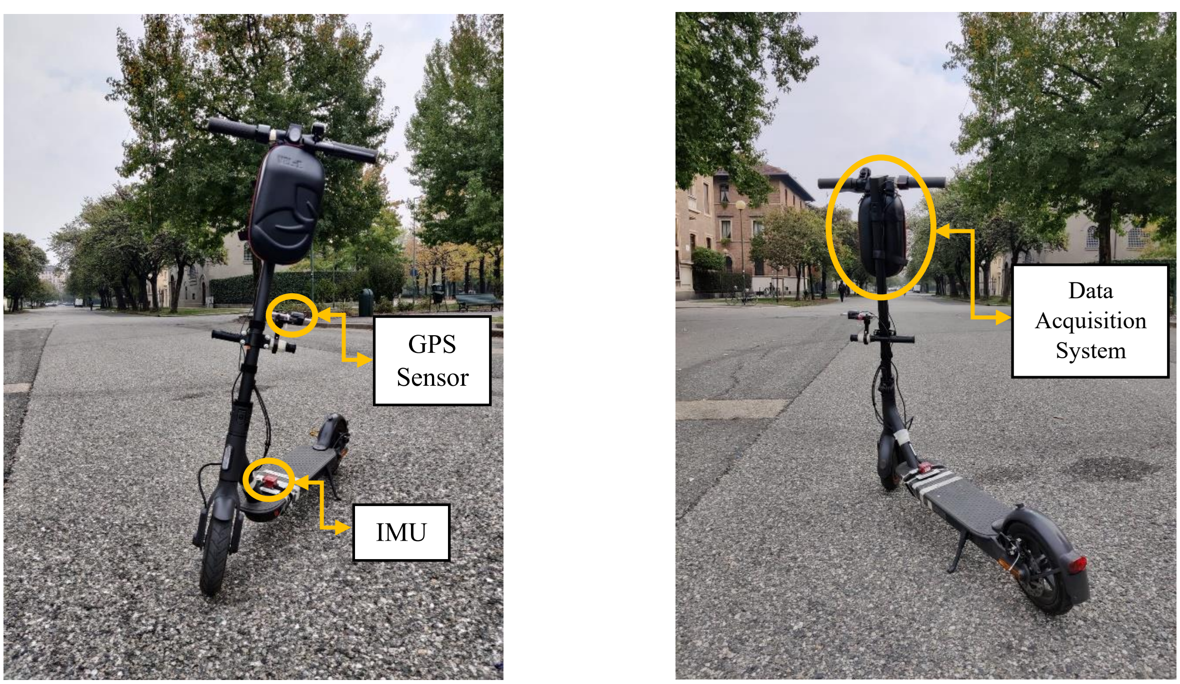

Figure 2.1.1 – The complete setup; front view (left) and rear view (right)

2.1.1 Inertial Measurement Unit

The IMU used in the thesis was Ellipse-A from SBG Systems. An IMU is sued to measure the acceleration, angular rates, and magnetic field in three dimensions. The Ellipse-A version is an attitude and Heading Reference System (AHRS), providing accurate orientation in dynamic conditions. The technical specifications for the IMU can be seen in Table 2.1.1.1. The mounting position of the sensor is underscored in Figure 2.1.1.1.

The Scadas XS resamples the sampling frequency of the IMU at 200 Hz irrespective of the sampling frequency set for the IMU in its setting.

Figure 2.1.1.1 – IMU mounted on the platform

Table 2.1.1.1 – Technical Specifications of Ellipse-A

	Unit	**Value**
	Accelerometer	
Vibration Rectification Error	μg/g^2	50
Bandwidth	Hz	390
Sampling rate	kHz	4
Orthogonality	°	0.05

Gyroscope		
Vibration Rectification Error	°/h/g^2	<1
Bandwidth	Hz	133
Sampling rate	kHz	10
Orthogonality	°	0.05

2.1.2 GPS Sensor

In order to record the velocity of the e-scooter and also, measure the distance travelled, a GPS sensor was used. Figure 2.1.2.1 shows the GPS sensor mounted on the steering rod using an external balance.

The additional weight of the balance was noted to be **263.4 grams** and was considered during further calculation. The GPS sensor is marked within a yellow circle in the figure shown below. The frequency of the GPS sensor was calculated to be 4 Hz.

Figure 2.1.2.1 – GPS sensor mounted over added balance

2.1.3 Proximity Sensor

The type of proximity sensor used is inductive type as it reacts to a metal surface, in our case, it is a set of 5 screws placed equidistance from the centre of the wheel as shown in Figure 2.1.3.1. The proximity sensor is responsible for capturing the pulses (from coming in contact with the screws) of rotating device. These pulses generate a voltage corresponding to the set value and the maximum voltage of the battery used to power the sensor. The voltage is then used to calculate the rpm of the rotating device.

The addition of the proximity sensor was to ensure the similarity of the vehicle speed with respect to the GPS sensor as well as the in-built speedometer of the e-scooter. The mounting of the sensor is shown in the figure below.

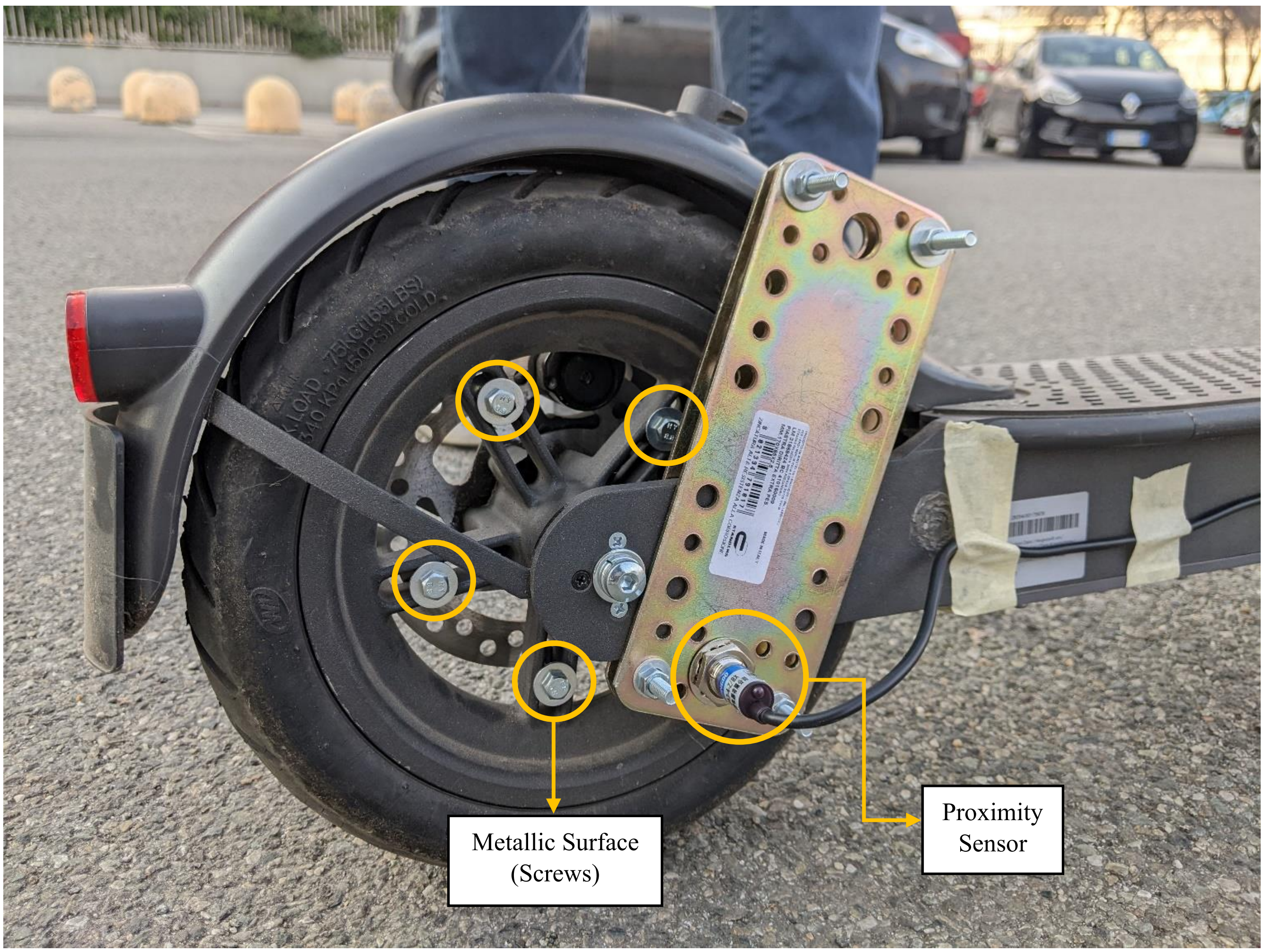

Figure 2.1.3.1 – Proximity sensor mounted on the rear wheel

2.1.4 Data Acquisition System

The data acquisition system is a device that stores the data signals coming from different sensors connected to the system. The data acquisition system used was Simcenter Scadas XS, which is a handheld recorder and front-end in one, and records predefined measurement data onto a removable micro SD card. It can operate in front-end mode, i.e. connected to a PC that runs Simcenter Testlab, or as a stand-alone recorder.

Figure 2.1.4.1 – Data acquisition system; Siemens Scadas XS (left) and case for Scadas XS (right)

As illustrated in figures above, the sensors are connected to the data acquisition system (Scadas XS) and put inside the carry bag for mobility and the safety of the device. Other than sensors, a continuous power supply (battery) is required to keep the device running which also is connected and put inside the bag.

2.2 Preliminary Analysis

Before analyzing the dynamics of the e-scooter, it is mandatory to perform certain preliminary test to verify for any anomalies. The set-up includes the use of proximity sensors at the rear to compare the rpm obtained through the same and the GPS. A preliminary analysis is a mandatory procedure to define the test parameters and procedure. The mounting of the proximity sensor is depicted in Figure 2.1.3.1 from Chapter 2.1.3.

The preliminary test is carried out to validate any differences in data obtained through different sensors. The test was performed with different constraints and parameters which will be discussed thoroughly in the next section. Finally, the test parameters will be set to perform further analysis on the vertical dynamics of the e-scooter.

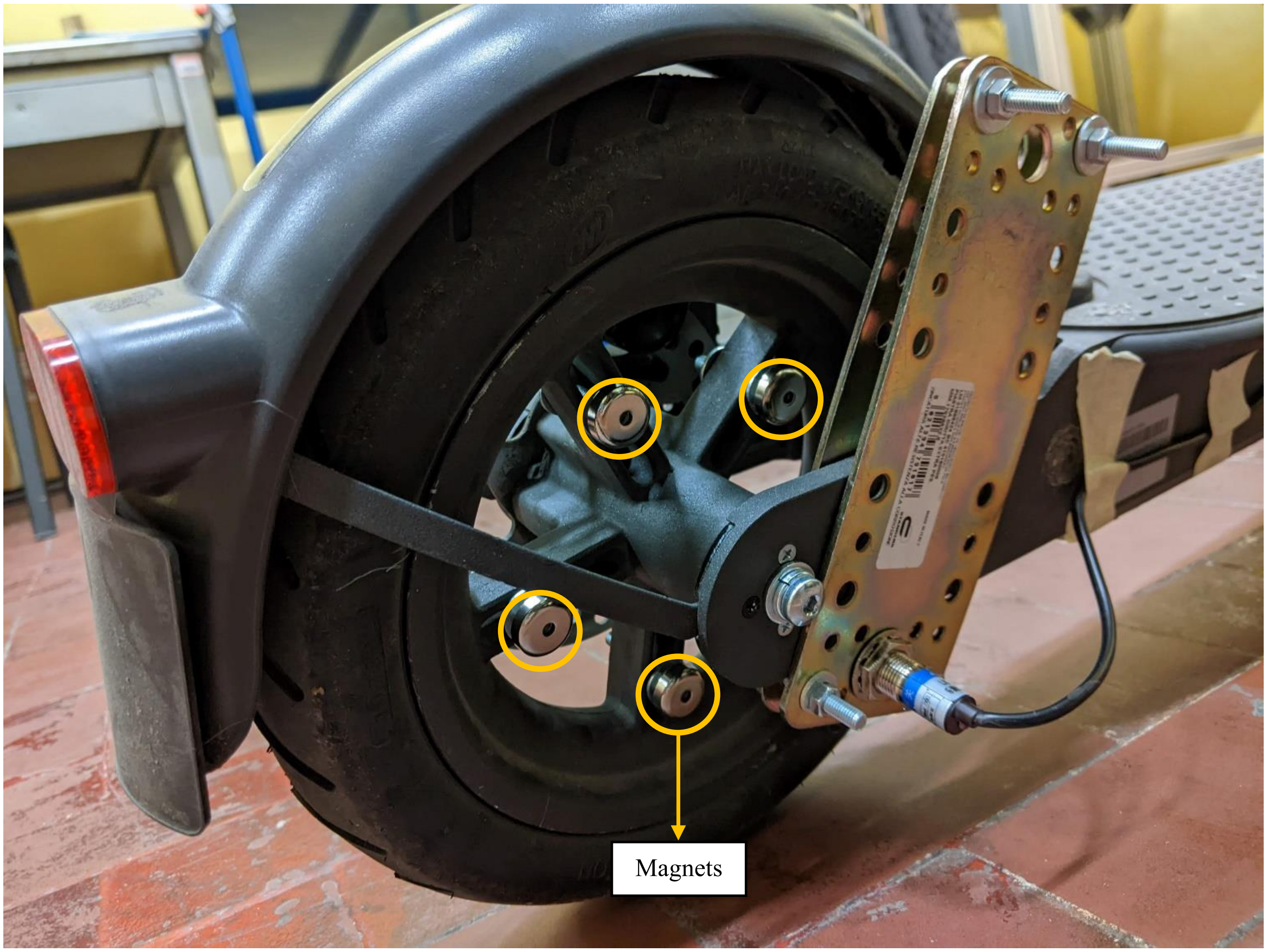

Figure 2.2.1 – Set-up with proximity sensor (with magnets)

To provide signal to the proximity sensor, metallic bolts were added as shown in Figure 5.1 to acquire pulses as the wheel rotates. There are 5 screws placed along the rim of the wheel which are responsible for providing pulses. Additionally, 5 set of magnets are added over the screws to compare any differences between both the set-ups, viz. with/without magnets. The mounting of magnets is shown in Figure 2.2.2 above.

From the experimental analysis, the signals acquired from both the set-ups, i.e. with and without magnets, were alike. Thus, the following tests were performed without the use of magnets.

2.2.1 Voltage

The battery used to power the proximity sensor has a maximum voltage of 7V. As seen in Figure 2.2.1.1, the pulses from different trigger voltages are similar to each other. But the trigger voltage plays an important role in the data acquisition. The difference in rpm data can be clearly seen in Figure 2.2.1.2.

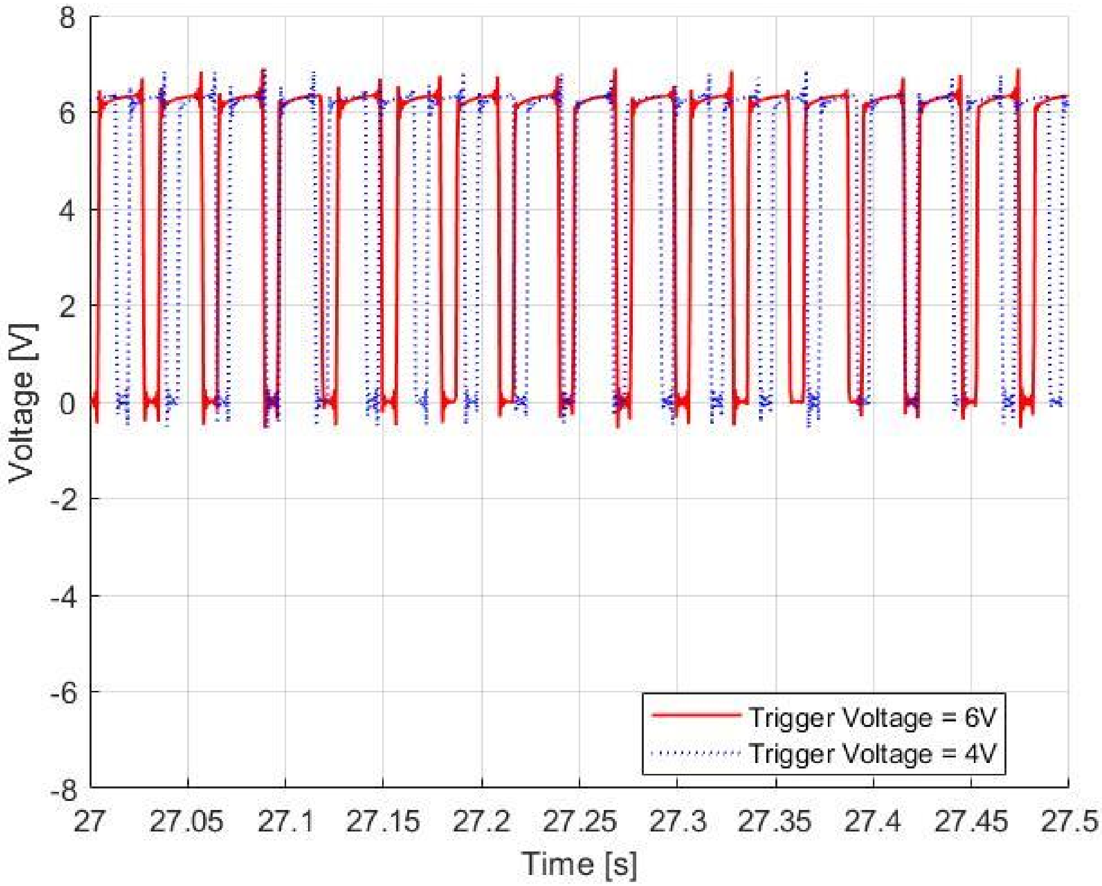

Figure 2.2.1.1 – Voltage Comparison

The parameters set for both the tests were kept constant with the trigger voltages being altered as discussed earlier. In Figure 2.2.1.2, the RPM data has a major difference which can be clearly noticed. This phenomenon is explained in Figure 2.2.1.3.

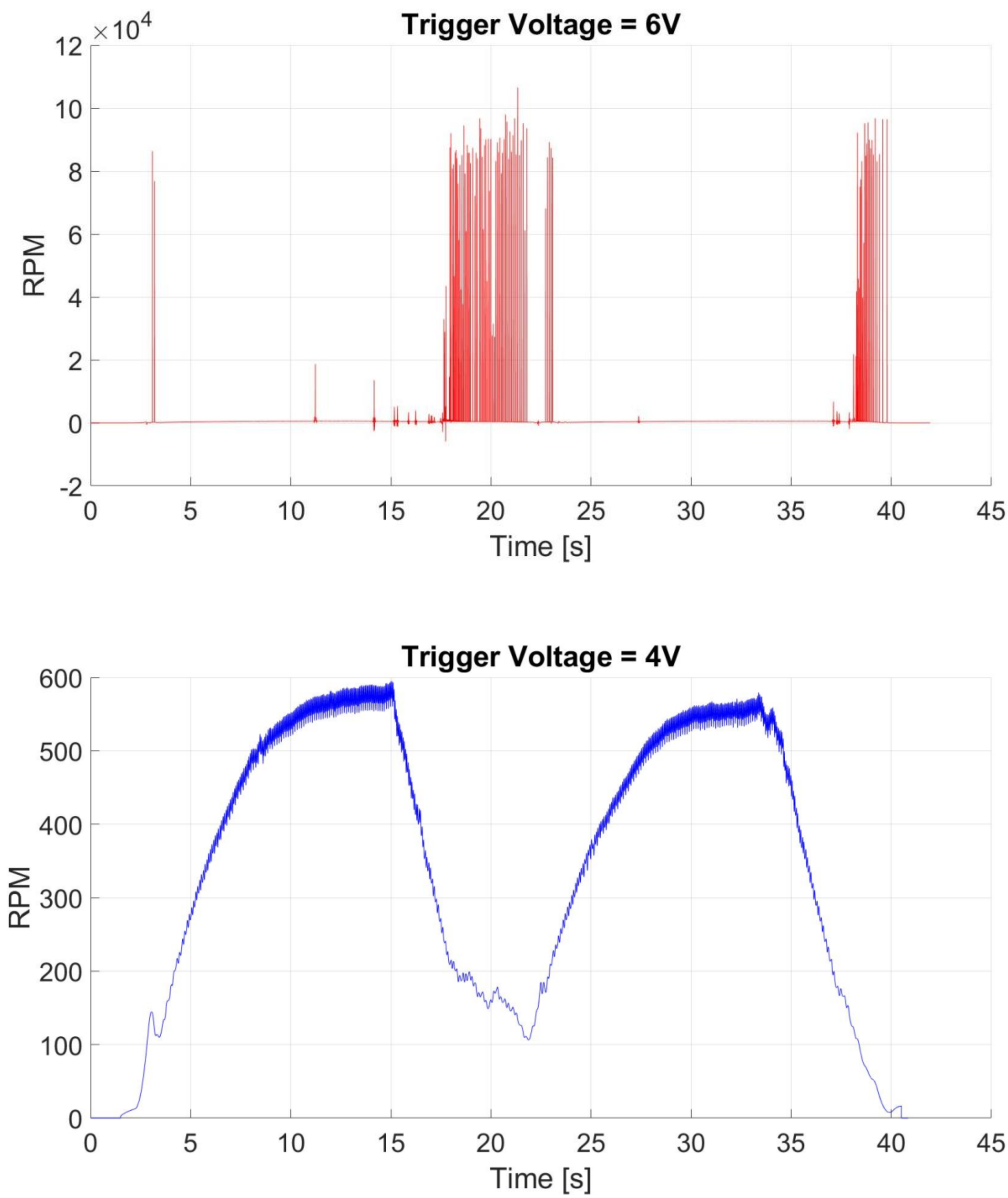

Figure 2.2.1.2 – Data acquired with trigger voltage = 6V (top) and data acquired with trigger voltage = 4V (bottom)

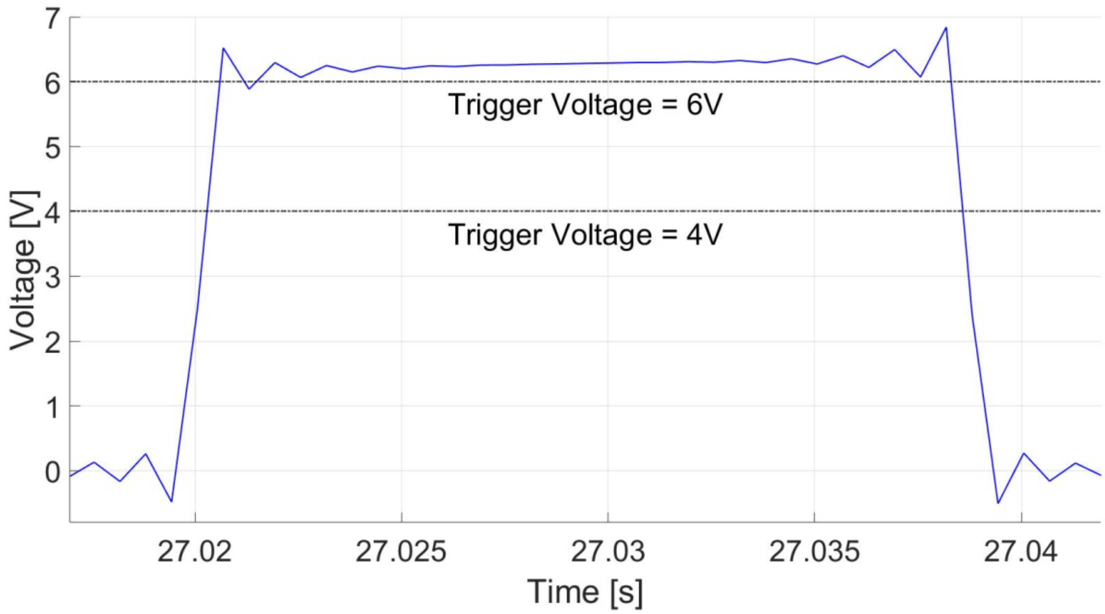

Figure 2.2.1.3 – Voltage Pulse

The figure shown above represents a pulse of voltage acquired from the proximity sensor at a randomly chosen time interval. At 6V, the intersection takes place more than two times as compared to 4V. This is true for all the pulses as shown in Figure 2.2.1.1. Thus, the RPM data acquired is non-uniform for trigger voltage = 6V as shown in Figure 2.2.1.2.

2.2.2 Cut-off Frequency

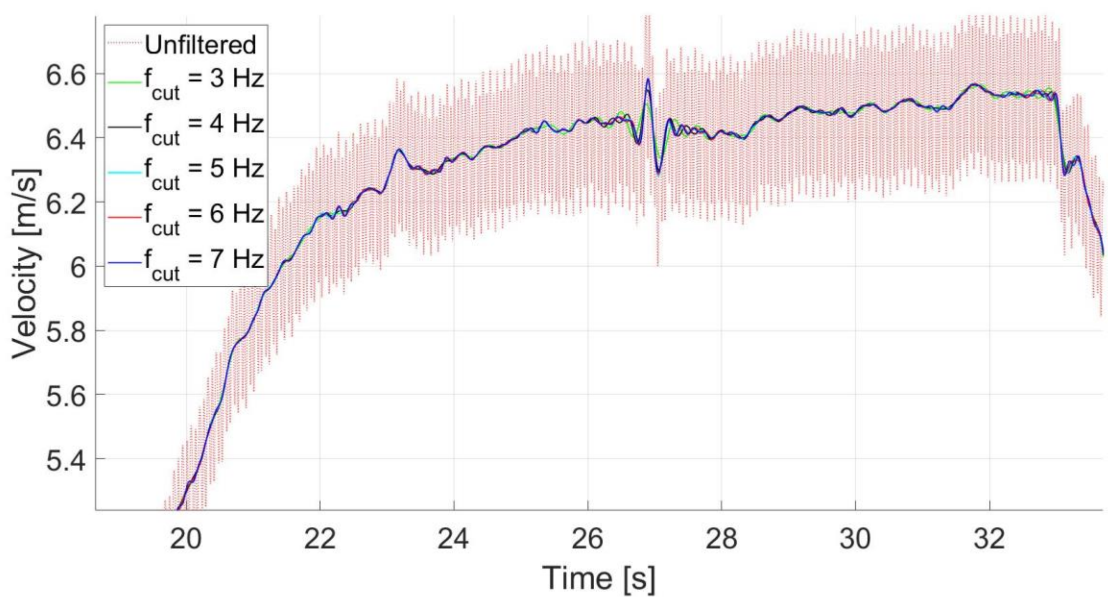

Figure 2.2.2.1 – Cut-off Frequency

A cut-off frequency is selected in such a way that the signal has a smooth transition from a high frequency interference to the low frequency information. Figure 2.2.2.1 depicts different cut-off frequencies for the same signal. It can be clearly seen that a cut-off frequency between 4 Hz and 6 Hz is a good fit. This range gives useful information for processing avoiding any high frequency interference.

2.2.3 Velocity

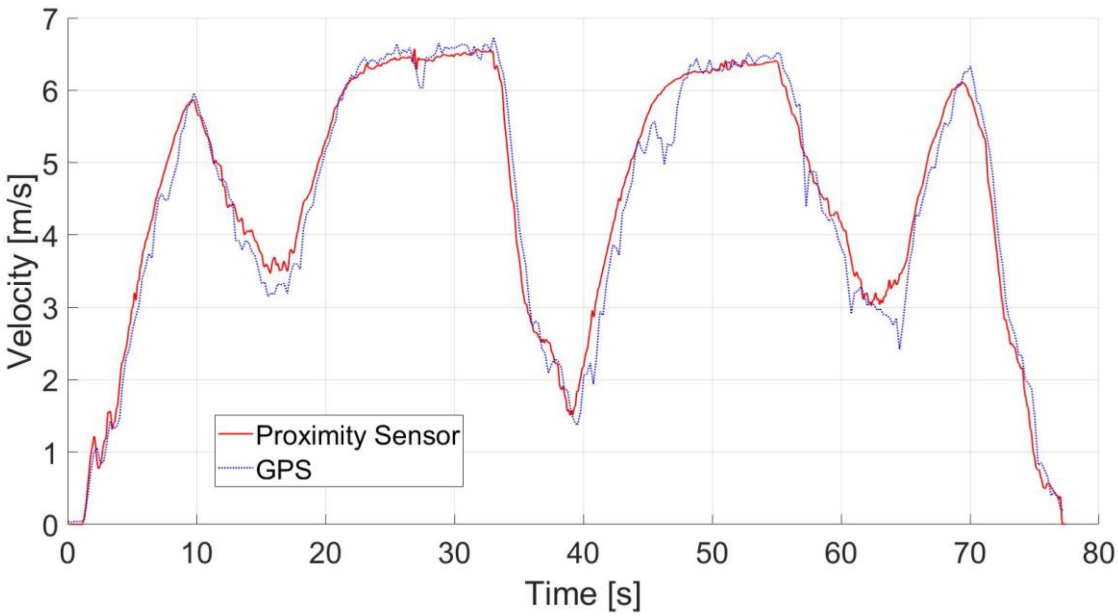

Figure 2.2.3.1 – Velocity Tracking

The velocity of the e-scooter over the duration of the test is depicted in Figure 2.2.3.1. The red solid line and the blue dotted line represent the velocities obtained from the proximity sensor and the GPS respectively. Both the velocities obtained are similar to each other except for few time periods where the GPS signal drifts away from the velocity obtained from the proximity sensor. This phenomenon can be explained with Figure 2.2.3.2 which represents the number of satellites available for the GPS sensor during the test period.

A higher value of 7 for the number of satellites shown in Figure 2.2.3.2 is a good number for the estimation of the velocity of the e-scooter. For the duration between 30 seconds and 40 seconds, the number of satellites recorded is 5 as seen in the figure. An enlarged figure (Figure 2.2.3.3) is illustrated in corresponding to Figure 2.2.3.1 for the same time interval. It can be clearly seen that GPS velocity drifts away more often than the velocity obtained from the proximity sensor.

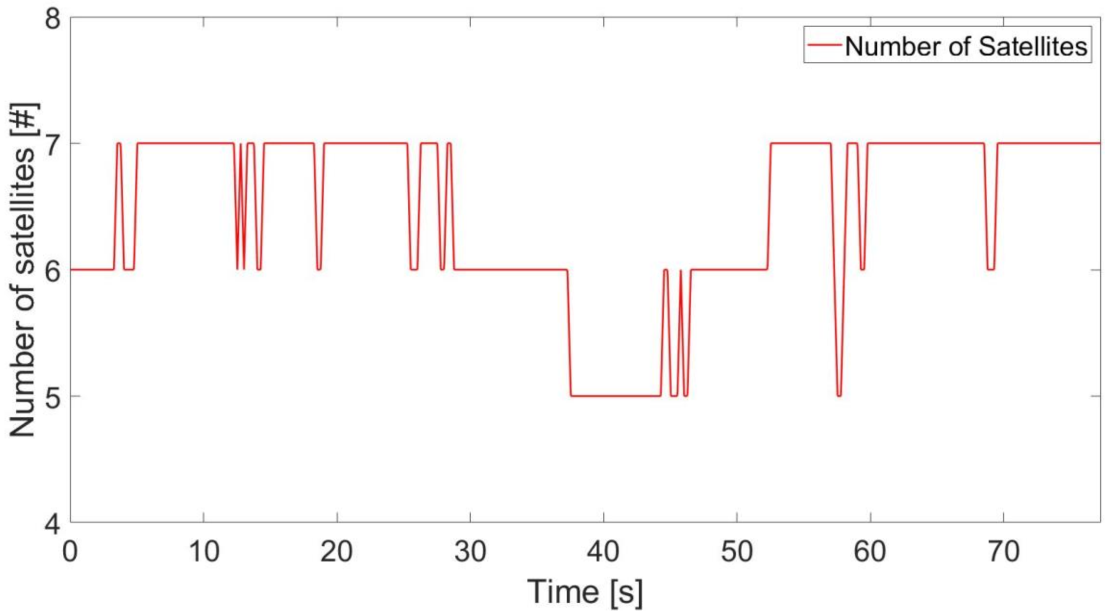

Figure 2.2.3.2 – Number of Satellites

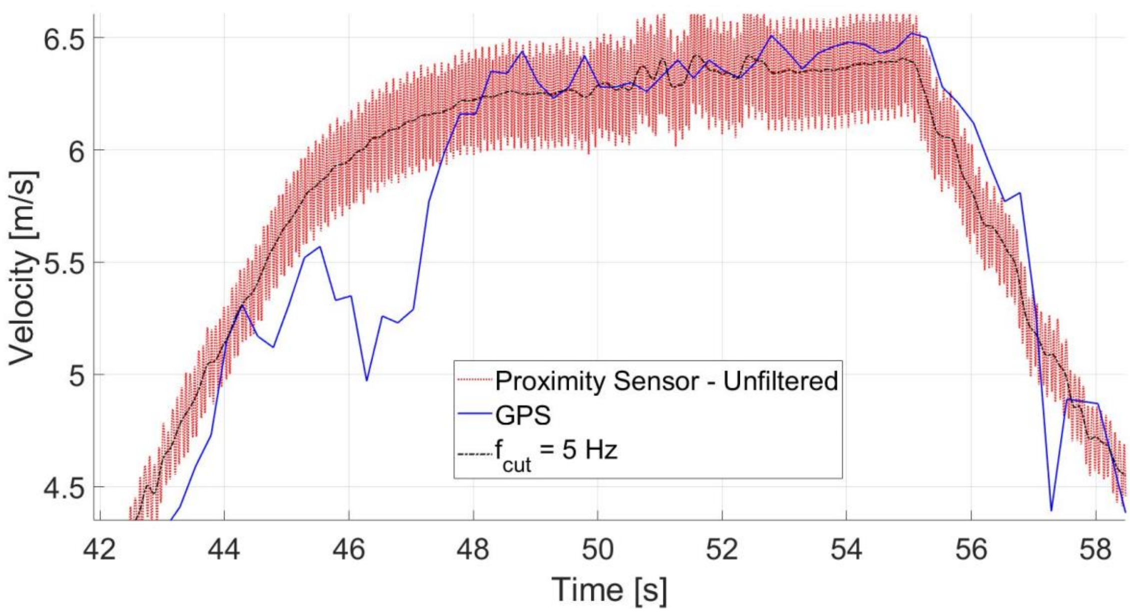

Figure 2.2.3.3 – Velocity Comparison

It can be concluded that the signal obtained from the GPS is not as uniform as the signal obtained from the proximity sensor. Despite being able to provide absolute location, the GPS gets updated less frequently which is why there are non-uniformities in the signal as shown in Figure 5.3.3 leading to inaccurate results. Therefore, the proximity sensor is more reliable than the GPS for velocity tracking.

3. Longitudinal Dynamics

3.1 Acceleration Test

3.1.1 Description of the task

The participant performed various tests and the different maneuvers and was supposed to keep the yaw rate as steady as possible during the entire duration of the test.

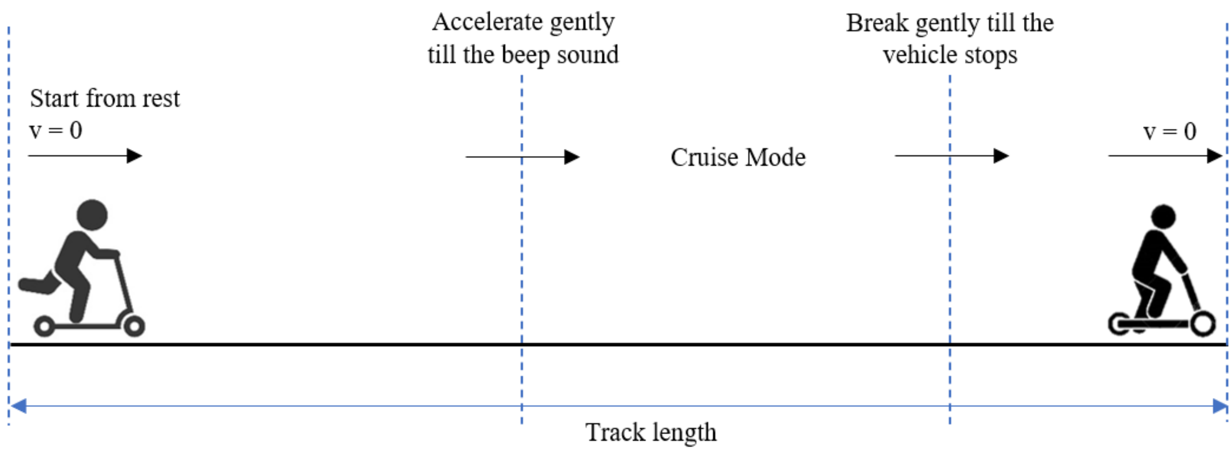

Figure 3.1.1.1 – Representation of the test run

The task was to study the behavior of vehicle acceleration in a straight road following the instructions as shown in Figure 3.1.1.1. It starts with the rider accelerating gently until a beep sound is heard after the velocity is kept constant for 2-3 seconds. The rider should accelerate until the maximum velocity is reached. A beep sound indicates the activation of the cruise mode. After few seconds of cruise mode, the rider is supposed to break gently until stoppage of the e-scooter.

The test was performed with two different footing locations which was marked with paper tape on the platform of the e-scooter as shown in Figure 3.1.1.2. The measurements are tabulated in Table 3.1.1.1.

Table 3.1.1.1 – Measurement of different configurations

Feet Location	**Reference Point**	**Distance [mm]**
Front	Front wheel centre	333
	Rear wheel centre	535
Rear	Front wheel centre	390
	Rear wheel centre	484

Figure 3.1.1.2 – Foot location configurations

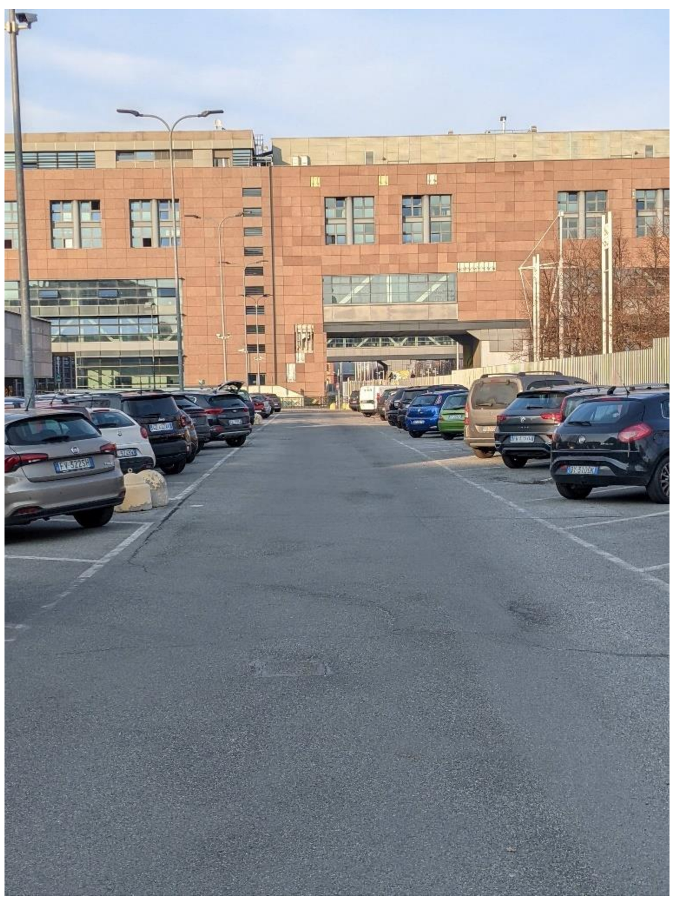

Figure 3.1.1.3 – Test track

3.1.2 Evaluation

For a better analysis of the acceleration of the e-scooter, various tests runs were performed out of which few tests are depicted in Figure 3.1.2.1. The figure illustrates the similarity between each test. It can be clearly seen that the tests are repeatable. The parameters for the tests shown in Figure 3.1.2.1 are drive mode with front feet configuration.

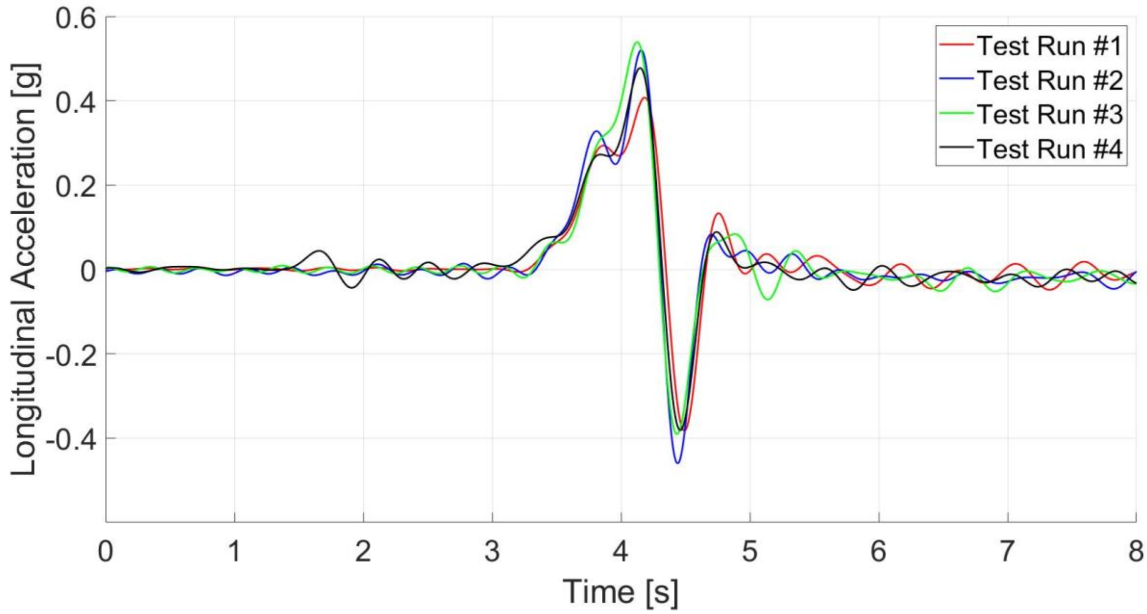

Figure 3.1.2.1 – Drive Mode; Front feet configuration

There is an increase in the acceleration between durations 3 seconds and 5 seconds. The positive slope depicts the acceleration of the e-scooter followed by constant velocity *($a_x \rightarrow 0\ m/s^2$)* approximately after 5 seconds. This shows the cruise mode as specified in Section 4.3.1 for the description of the task.

Apart from the feet location as a parameter as mentioned in Table 3.1.1.1, the test was performed in two different modes available in the e-scooter. The drive mode enables the rider to reach a maximum speed of 20 km/h while the sport mode has a maximum velocity of 25 km/h.

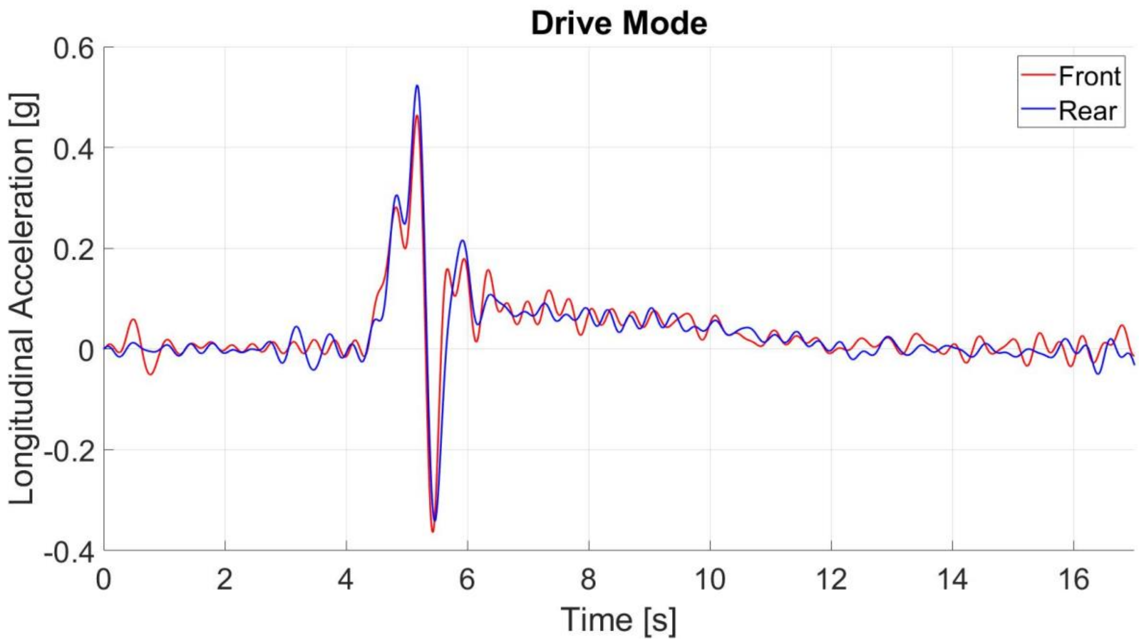

Figure 3.1.2.2 – Front and Rear configurations (Drive Mode)

With reference to Table 3.1.1.1, the red line and the blue line represent the front and the rear configurations respectively as shown in Figure 3.1.2.2 and Figure 3.1.2.3. There is a slight difference in the g-force during the acceleration phase because to the shift of centre of gravity location due to different footing locations. The acceleration stays in the range of ±0.6g. This effect is during the starting phase, i.e., during the kick phase to start the motor.

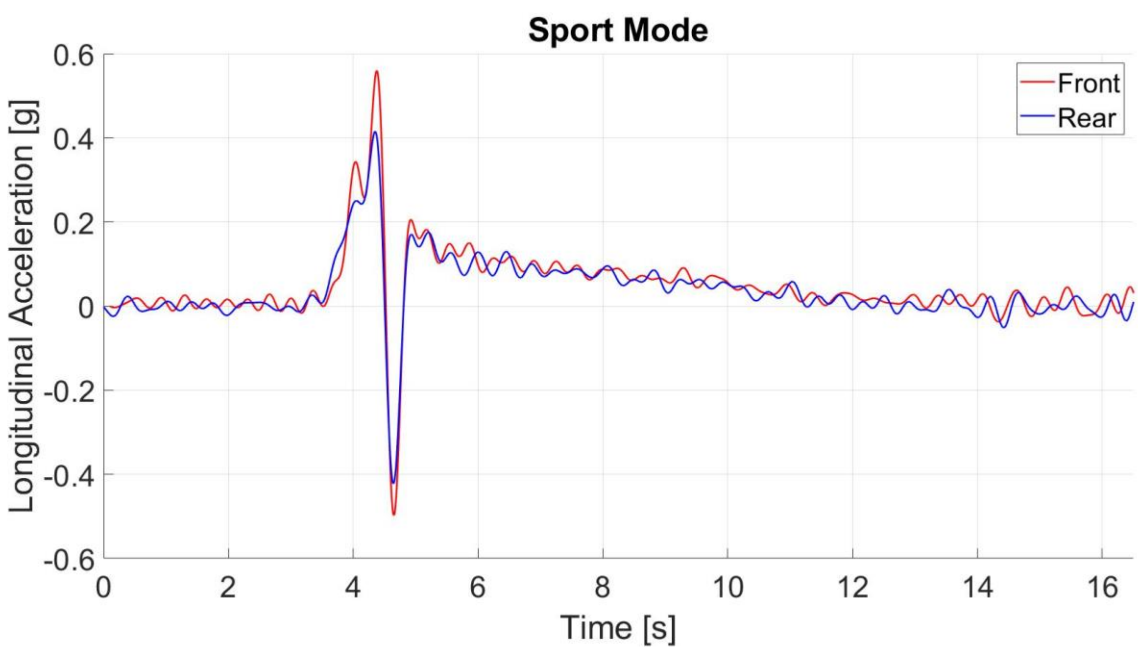

Figure 3.1.2.3 – Front and Rear configurations (Sport Mode)

Referring to Figure 3.1.2.3, the motor starts accelerating approximately after 4.5 seconds after reaching the minimum velocity required to start the motor. There is a constant acceleration phase between 6 and 12 seconds. The irregularity in the acceleration can be justified with the test track surface as the surface was not completely flat and had certain degree of elevation. The e-scooter then enters the cruise mode between 12 and 16 seconds as depicted in the figure.

The range of acceleration during the motor phase is between ±0.2g.

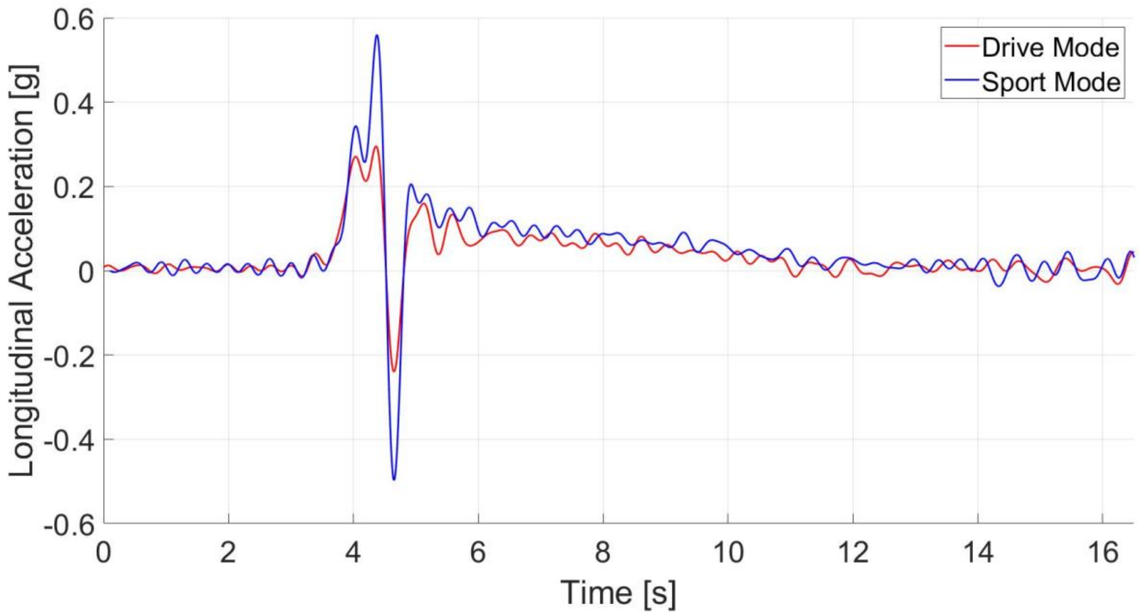

Figure 3.1.2.4 – Drive Mode and Sport Mode

As indicated in Figure 3.1.2.4, the difference in accelerations between the drive mode and the sport mode is not very large. It can be concluded that the sport mode has greater acceleration than the drive mode, but it is within the upper and lower limits of ±0.2g.

By comparing the figures mentioned above, it can be clearly seen that the maximum acceleration takes place in the direction of motion of the vehicle, i.e. x-axis of the vehicle within the range of [-0.2 0.2]g during the motoring phase.

3.2 Brake Test

3.2.1 Description of the task

The description for brake test is similar to the acceleration test performed in Chapter 3.1 except for the stoppage of the vehicle. The participants were instructed to hard brake instead of gentle braking after reaching the cruise mode and maintaining the velocity for 2-3 seconds.

The task was to study the acceleration due to braking and the braking distance which is discussed in detail in the next section. The illustration of the description of the task in demonstrated in Figure 3.2.1.1.

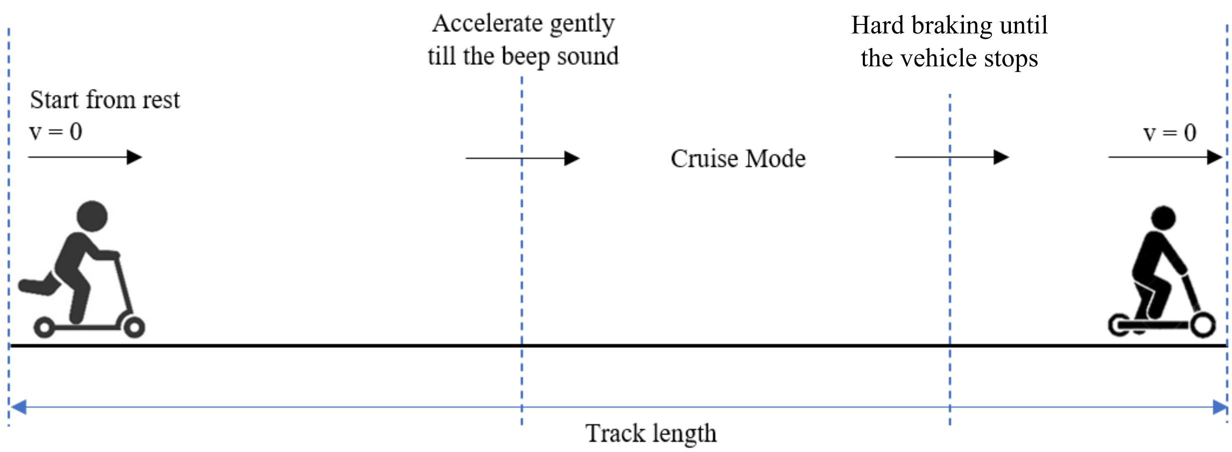

Figure 3.2.1.1 – Description of the task

The test was performed in the same track where the acceleration test was performed. It is depicted in Figure 3.1.1.3 in Chapter 3.1.1.

3.2.2 Evaluation

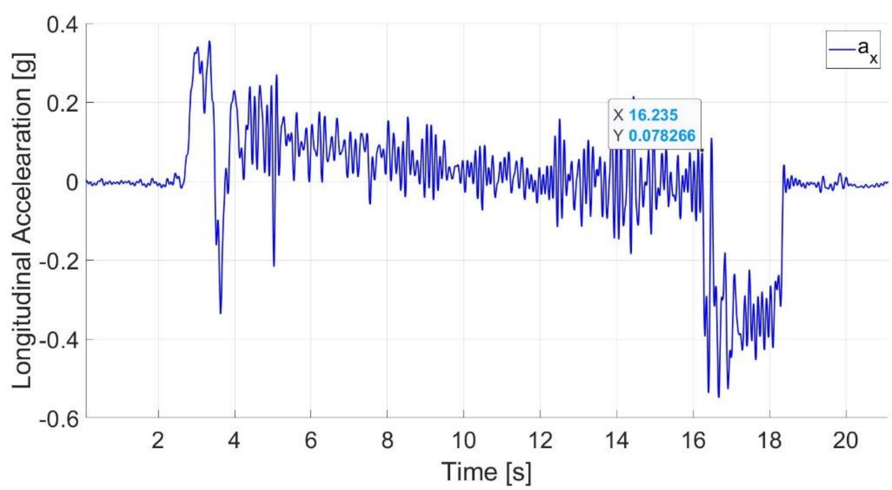

Figure 3.2.2.1 – Braking

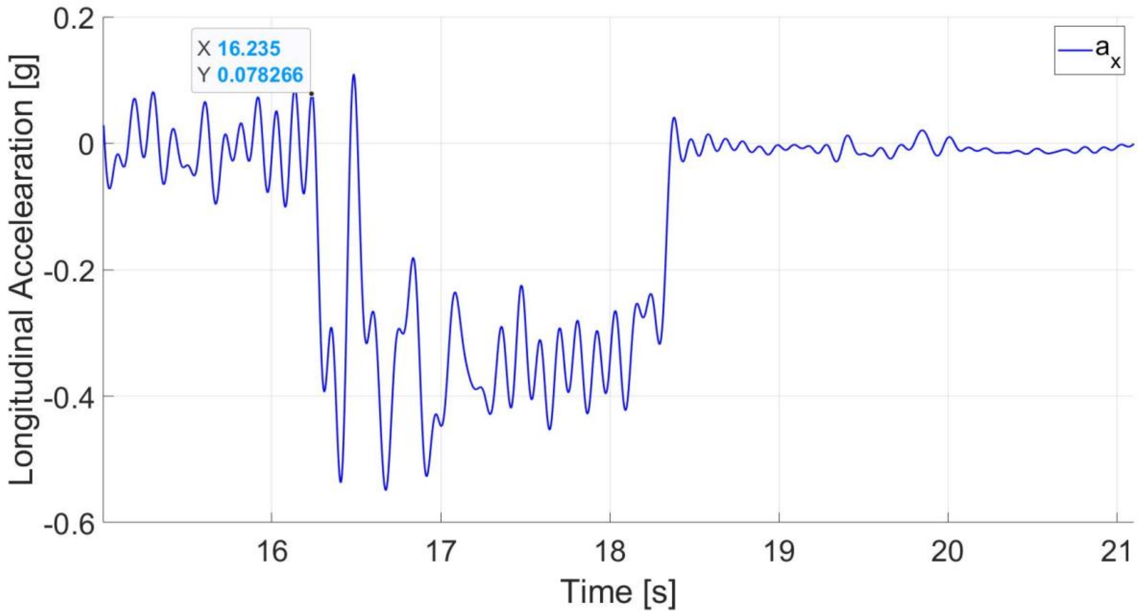

Figure 3.2.2.2: Braking (enlarged)

In Figure 3.2.2.1, the acceleration during the test duration is illustrated. As shown with a data tip, the hard braking begins at 16.235 seconds after which there is a sudden negative acceleration, i.e. braking. A clearer depiction of the braking phenomenon is shown in Figure 3.2.2.2. The maximum force observed is less than (-0.6)g.

The braking distance is calculated as the distance travelled by the e-scooter between the velocities 5 m/s and 0 m/s.

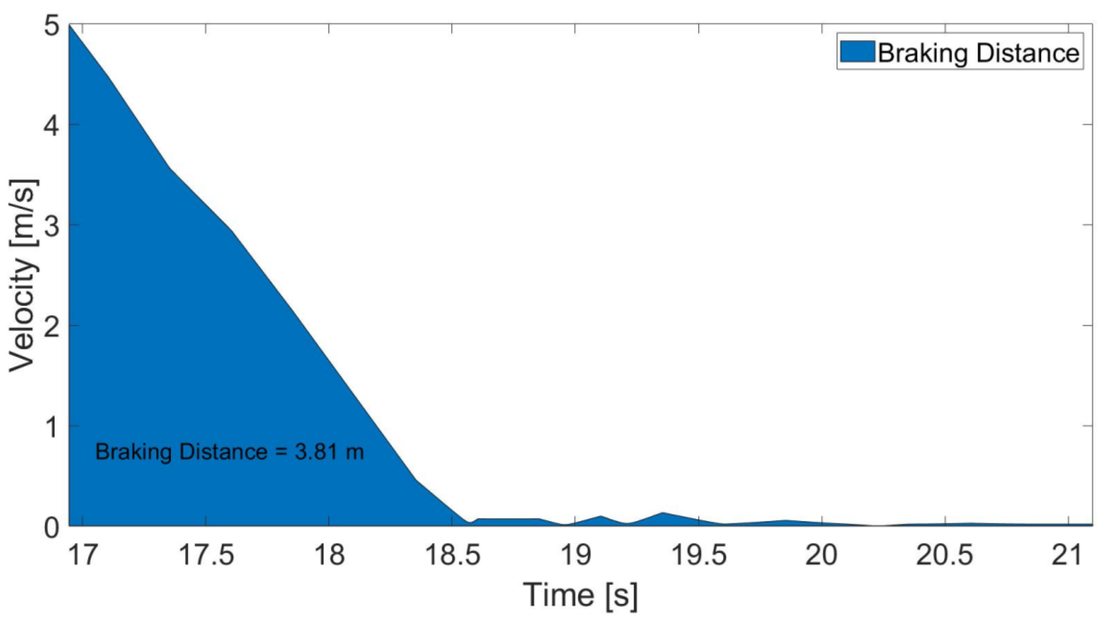

Figure 3.2.2.3 – Velocity-Time Graph

The braking distance for various tests is tabulated in Table 3.2.2.1 and Table 3.2.2.2 with different parameters and, it is also graphically illustrated in Figure 3.2.2.3 for one of the test-runs from the table. The velocity-time graph is depicted in Figure 3.2.2.3 which shows the braking distance under the area of the curve.

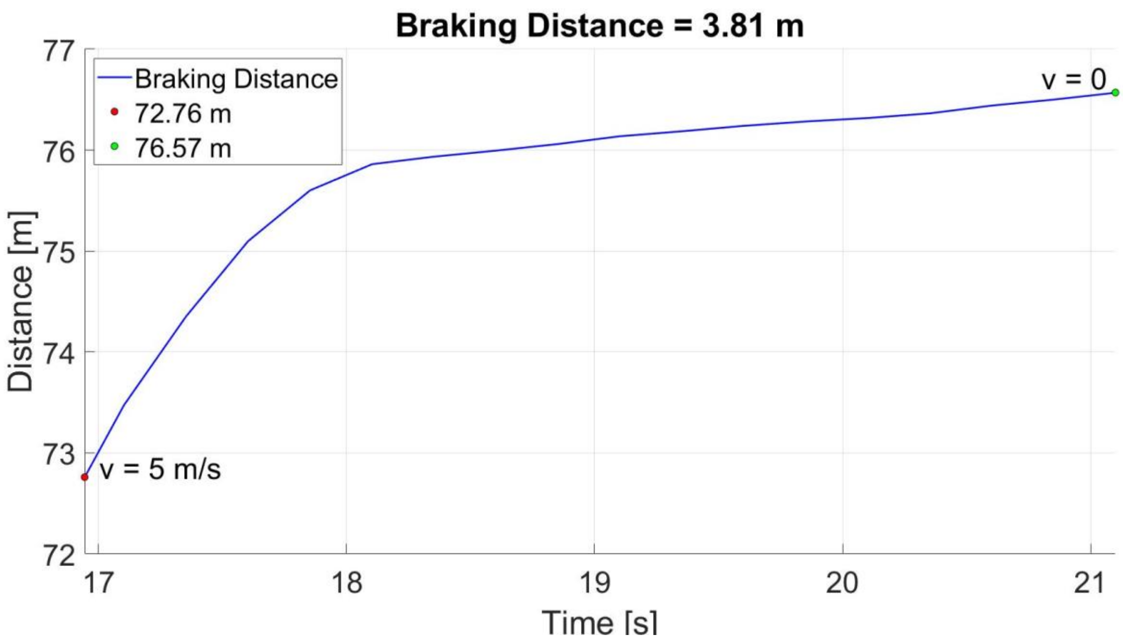

Figure 3.2.2.4 – Cumulative Braking Distance

The figure depicted above displays the cumulative braking distance labelled with the start and end points of the brake test of the velocity-time graph of the same test from Figure 3.2.2.3.

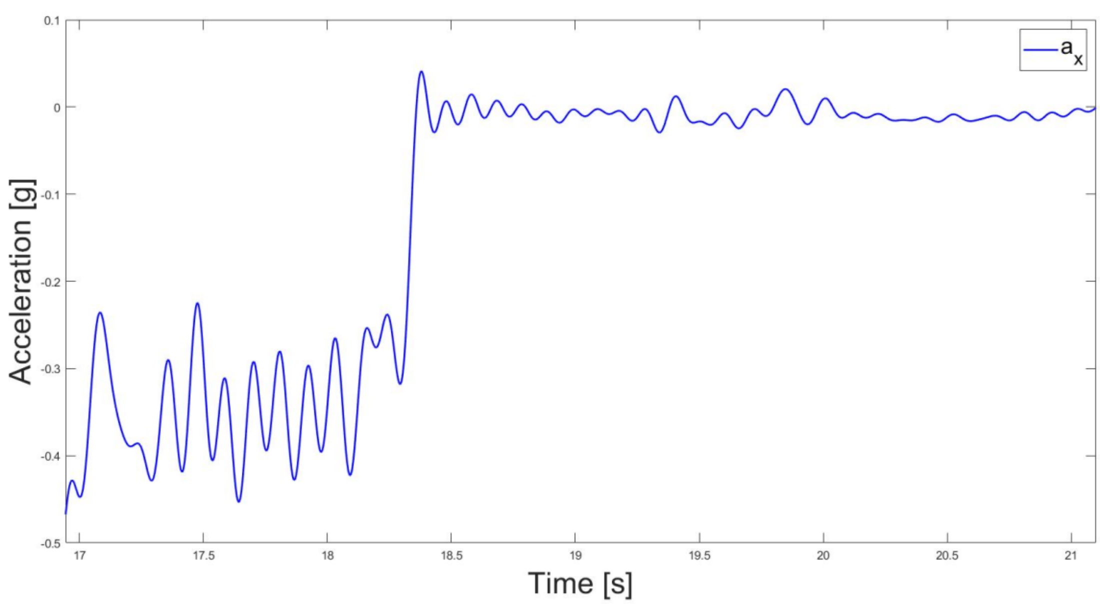

Figure 3.2.2.5 – Acceleration due to braking

With reference to the velocity-time plot depicted in Figure 3.2.2.3, the figure shown above illustrates the corresponding acceleration due to braking during the period when the e-scooter is between the velocities 5 m/s and 0 m/s.

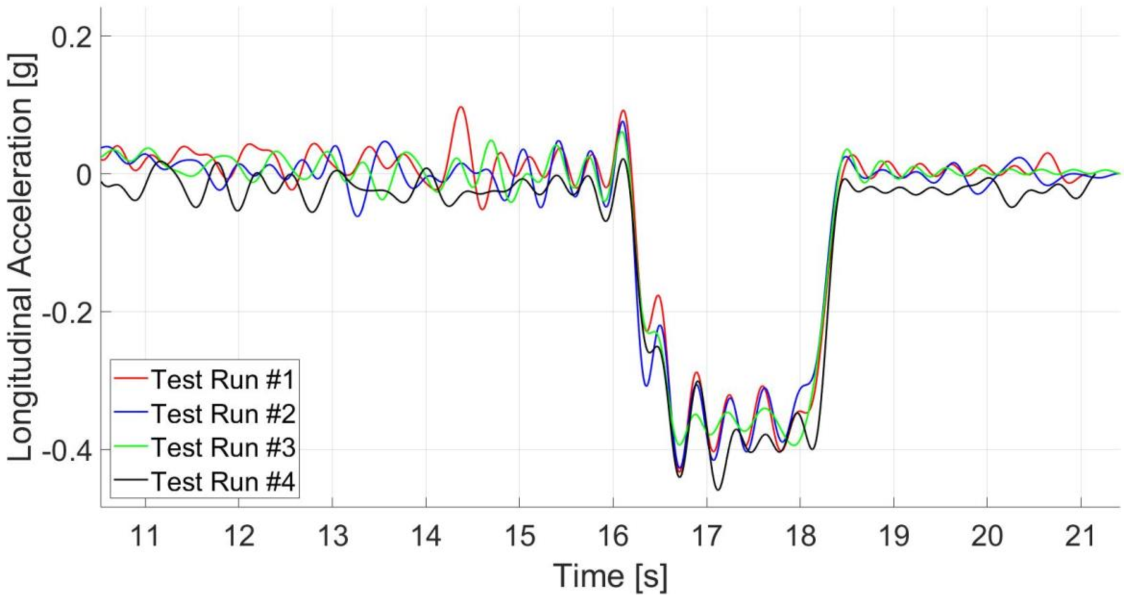

Figure 3.2.2.6 – Sport Mode: Rear feet configuration

Figure 3.2.2.6 demonstrates the repeatability of the test procedure. Four tests driven with sport mode were chosen randomly with the rear feet configuration as shown in the figure above. The negative slope in the figure depicts the deceleration (braking) of the e-scooter at about 16 seconds followed by $a_x \rightarrow 0$ m/s^2 which implies the stoppage of the e-scooter at about 21.5 seconds.

Table 3.2.2.1 – Braking Distance: Rider Weight ≈ 80 kg

Tyre Pressure [bar]	**Regeneration Mode**	**Braking Distance [m]**	**Average Braking Distance [m]**
2.5	Low	6.11	4.53
		3.95	
		4.69	
		4.09	
		3.79	
3.5	Low	3.24	3.62
		3.70	
		3.81	
		3.60	
		3.76	

	Medium	4.71	3.57
		3.43	
		3.11	
		3.37	
		3.22	
	High	3.30	3.22
		3.97	
		2.75	
		3.04	
		3.03	
4.5	Low	4.07	4.12
		3.68	
		4.06	
		4.73	
		4.08	

Table 3.2.2.2 – Braking Distance: Rider Weight ≈ 85 kg

Tyre Pressure [bar]	**Regeneration Mode**	**Braking Distance [m]**	**Average Braking Distance [m]**
2.5	Low	4.51	3.62
		3.19	
		3.58	
		3.77	
		3.05	
3.5	Low	2.56	3.28
		3.05	
		3.24	
		3.63	
		3.93	
	Medium	2.90	3.22
		3.42	
		3.49	
		2.95	
		3.34	
	High	3.15	3.18
		3.02	
		3.59	
		2.85	
		3.28	

4.5	Low	4.01	3.58
		3.33	
		3.80	
		3.20	
		3.56	

Table 3.2.2.3 – Braking Distance: Rider weight ≈ 82 kg

Tyre Pressure [bar]	**Regeneration Mode**	**Braking Distance [m]**	**Average Braking Distance [m]**
3.5	Low	3.53	3.53
		3.58	
		3.10	
		3.66	
		3.77	

Table 3.2.2.4 – Braking Distance: Rider weight ≈ 90 kg

Tyre Pressure [bar]	**Regeneration Mode**	**Braking Distance [m]**	**Average Braking Distance [m]**
3.5	Low	2.83	2.76
		2.57	
		3.02	
		2.85	
		2.53	

Table 3.2.2.5 – Braking Distance: Rider weight ≈ 93 kg

Tyre Pressure [bar]	**Regeneration Mode**	**Braking Distance [m]**	**Average Braking Distance [m]**
3.5	Low	2.54	2.44
		2.48	
		2.84	
		2.22	
		2.12	

The braking test was assessed considering the following parameters:

- Tyre Pressure
- Regeneration Mode
- Rider Weight

Tyre Pressure

As tabulated in Table 3.2.2.1 and Table 3.2.2.2, the braking distances for various test runs are different. Although the braking force is within ±0.6g, tyre pressure plays a significant role in the braking distance. The braking distances with tyre pressures 2.5 bar and 4.5 bar is comparatively more with tyre pressure 2.5 bar. This can be explained by underinflation and overinflation of the tyres at 2.5 bar and 4.5 bar, respectively. During such phenomenon, the contact patch available for braking is less as compared to the e-scooter with tyre pressure 3.5 bar. Therefore, having the right amount of tyre pressure is necessary for braking.

Regeneration Mode

There were three regeneration mode settings available in MI Pro 2, namely, low, medium, and high. The braking distance reduces as the regenerative mode is increased. With high setting, the motor of the e-scooter rotates faster in the opposite direction as compared to the low settings. Thus, the braking distance is less with high regeneration mode.

The results are tabulated in Table 3.2.2.1 and Table 3.2.2.2.

Rider Weight

To assess the braking according to the rider weight, few of my colleagues were invited to perform the braking test and they were instructed to perform the test run according to the description discussed for the analysis. The weight of the riders ranged between 70 kg to 95 kg. The results are tabulated in Table 3.2.2.1 – Table 3.2.2.5.

The greater the weight of the rider, the more is the braking force available at the wheels to stop the vehicle. It implies that the larger the braking force, the shorter is the braking distance. It can be clearly seen from the tables above that the braking distance is the least for the rider with 80 kg of weight while it is the highest for the rider with 93 kg of weight.

3.3 Coastdown Test

The procedural techniques used in this test can be used to assess the impact of the vehicle attribute on coast down performance, and thus drag and rolling resistance. Test variables that have been used are tabulated with the results. As will be discussed in the following section, tire pressure has a significant effect on vehicle coastdown, well within the experimental variability.

It should be noted that changing the tire pressure affects the tires effective rolling radius. This can introduce experimental error into the data if the vehicles own speed sensing system is used to log data, as not in this case because a GPS sensor was used to determine the vehicle speed.

Basic equation for longitudinal dynamics is given by:

$$F_{trac} - F_{res} = m_e \frac{dv}{dt}$$

where,
F_{trac} = traction force available at wheel
F_{res} = total driving resistance
m_e = equivalent mass
$\frac{dv}{dt} = a$ = vehicle acceleration

$F_{trac} > F_{res}$ → The exceeding force is used to accelerate the vehicle

The total driving resisting can be computed as:

$$F_{res} = F_{aer} + F_{rol} + F_{cli}$$

where,
F_{aer} = aerodynamic resistance
F_{rol} = rolling resistance
F_{cli} = climbing resistance (due to the slope)
For the coastdown testing, the test track as shown in Figure 4.3.1.3 is almost flat. Therefore, the climbing resistance is neglected, i.e. $F_{cli} \rightarrow 0$. Thus, the equation gets reduced to:

$$-(F_{aer} + F_{rol}) = m_e \frac{dv}{dt} \quad \rightarrow \quad F_{cd} = -m_e \frac{dv}{dt}$$

where,
$m_e = m_r + m_v + m_{add}$
m_r = mass of rider
m_v = mass of vehicle
m_{add} = additional mass

Experimental measurements of vehicle speed, $v(t)$ as a function of time, t allows to calculate the coastdown resistance, F_{cd} for each value of vehicle speed, v.

From analytical point of view:

$$F_{cd} = F_{aer} + F_{rol} = \frac{1}{2}\rho S C_d v^2 + (B_0 + B_2 v^2) m_t g$$

ρ = air density [kg/m^3]
C_d = vehicle aerodynamic drag coefficient [-]
v = vehicle speed (relative to wind speed) [m/s]
S = vehicle cross section [m^2]
m_t = Vehicle mass
B_0 = Tyre coefficient due to static component
B_2 = Tyre coefficient due to viscous

Considering all the terms as a function of the vehicle speed, v:

$$F_{cd} = (B_0 m_t g) + \left(\frac{1}{2}\rho S C_d \frac{1}{3.6^2} + B_2 m_t g\right) v^2$$

And, from the above equation, it is expected that the experimentally measured F_{cd} should be well fitted by a quadratic regression of the vehicle speed, v. Performing a linear regression as a function of v^2, the following equation is obtained:

$$F_{cd} = R = A + Bv^2 \quad \rightarrow \quad -m_e \frac{dv}{dt} = A + Bv^2$$

Using this information, a polynomial regression model was devised in MATLAB and its corresponding function. The inputs for the function include the total inertia of the vehicle and the velocity of the vehicle as a function of time. The coastdown coefficients were calculated between the vehicle velocities, $v = 5$ m/s and $v = 2$ m/s. The results are tabulated according to the different parameters discussed above from Table 4.5.2 – Table 4.5.5.

Table 3.3.1 – Test information for Table 3.3.2

Wind Speed	**Temperature**	**Humidity**	**Drive Mode**	**Rider Weight**	**Effective Mass**	**Tyre Pressure**
3 km/h E	13° C	76%	Sport	80 kg	94.463	3.5 bar

Table 3.3.2 – Coastdown results (Regeneration mode)

Regeneration Mode	A	B
Low	3.335	0.04476
Medium	5.567	0.02704
High	8.296	0.02153

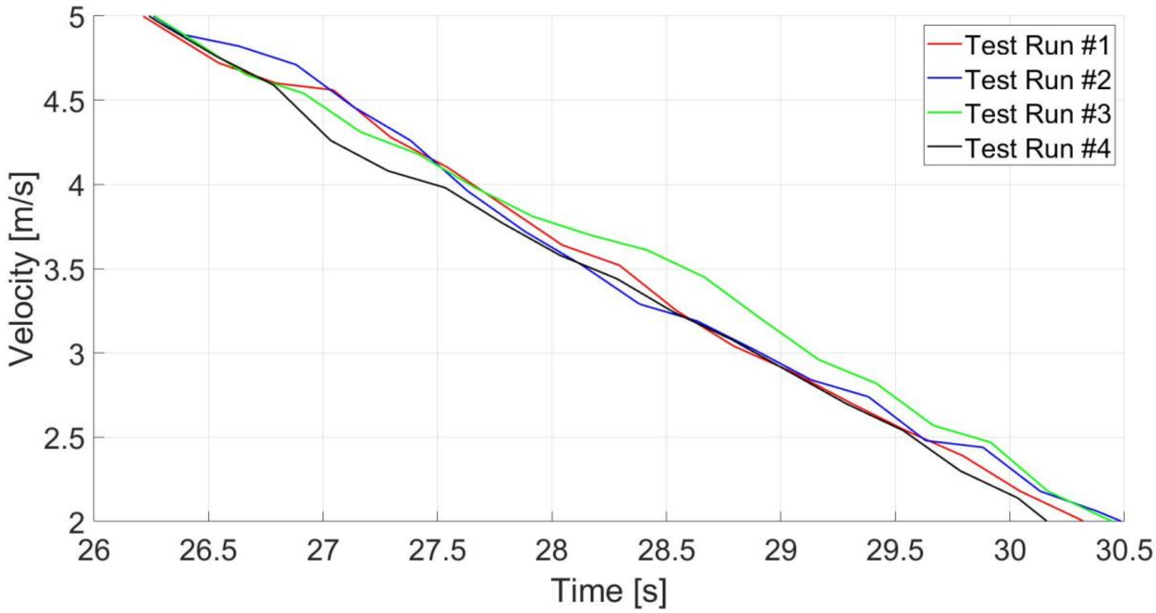

Figure 3.3.1 – An example of coasting data for medium regeneration mode

Table 3.3.3 – Test information for Table 3.3.4 and Table 3.3.5

Wind Speed	Temperature	Humidity	Drive Mode	Rider Weight	Effective Mass	Regeneration Mode
5 km/h S	14° C	81%	Sport	80 kg	94.463	Low

Table 3.3.4 – Coastdown results (Tyre pressure)

Tyre Pressure [bar]	A	B
2.5	3.804	0.04894
3.0	3.699	0.05257
3.5	3.249	0.06162
4.0	2.905	0.07575

Table 3.3.5 – Coastdown results (e-scooter off)

Tyre Pressure	A	B
3.5 bar	1.854	0.06006

For Table 3.5.5, the rider was supposed to reach the maximum velocity and enter the cruise mode of the e-scooter. After reaching the cruise mode, the scooter was turned off to nullify the effect of the regenerative braking feature of the e-scooter.

Table 3.3.6 – Test information for Table 3.3.7

Wind Speed	**Temperature**	**Humidity**	**Drive Mode**	**Rider Weight**	**Effective Mass**
4 km/h S	17°C	79%	Sport	85 kg	99.463 kg

Table 3.3.7 – Coastdown results

Regeneration Mode	**Tyre Pressure**	**A**	**B**
Low	3.5 bar	3.177	0.06088

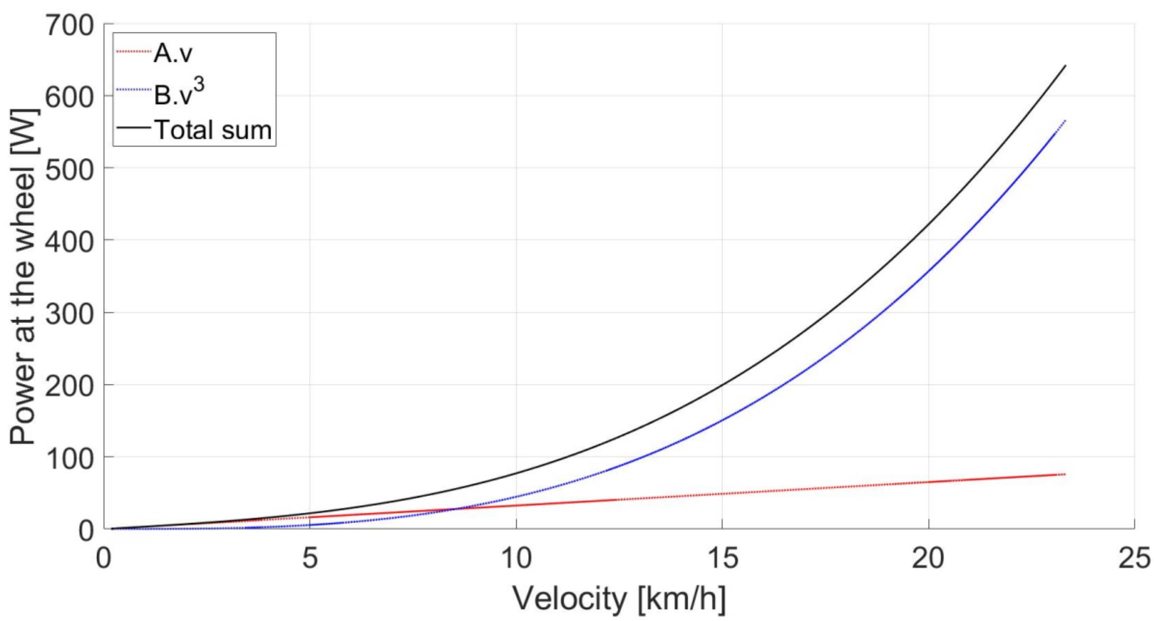

Figure 3.3.2 – Overall power vs velocity and specific contribution from coastdown coefficients

4. Vertical Dynamics

The ride comfort focuses on vehicle vibration and pitch movement caused by vertical tire motion.

Table 4.1 – Definition of parameters

Parameters	**Value**
Cut-off Frequency	5 Hz
Trigger Voltage	4 V
Magnets	No effect
Slope	Down

After the discussion of results from the preliminary analysis in Chapter 2.2, the ideal parameters required to proceed with the vertical dynamics have been tabulated in Table 4.1. These results will be used to perform various test runs for the study of vertical dynamics of the e-scooter.

Figure 4.1 – Accelerometers mounter at the centre of the front wheel (left) and at the center of the rear wheel (right)

4.1 Description of the task

Figure 4.1.1 represents the description of the task pictorially. The rider is supposed to accelerate the e-scooter up to 12 km/h and maintain the velocity to activate the cruise mode. Then, the rider should maintain the e-scooter steady as he/she passes the bump area as shown in Figure 4.1.1. After passing the bump area, the rider is supposed to break gently till the scooter stops.

The aim of the task is to analyze the force acting on the e-scooter while passing through the bump. As shown in the setup in Figure 4.1, accelerometers are mounted on different locations as marked in the figure. The forces acting on it will be compared and discussed in detail in the upcoming sections.

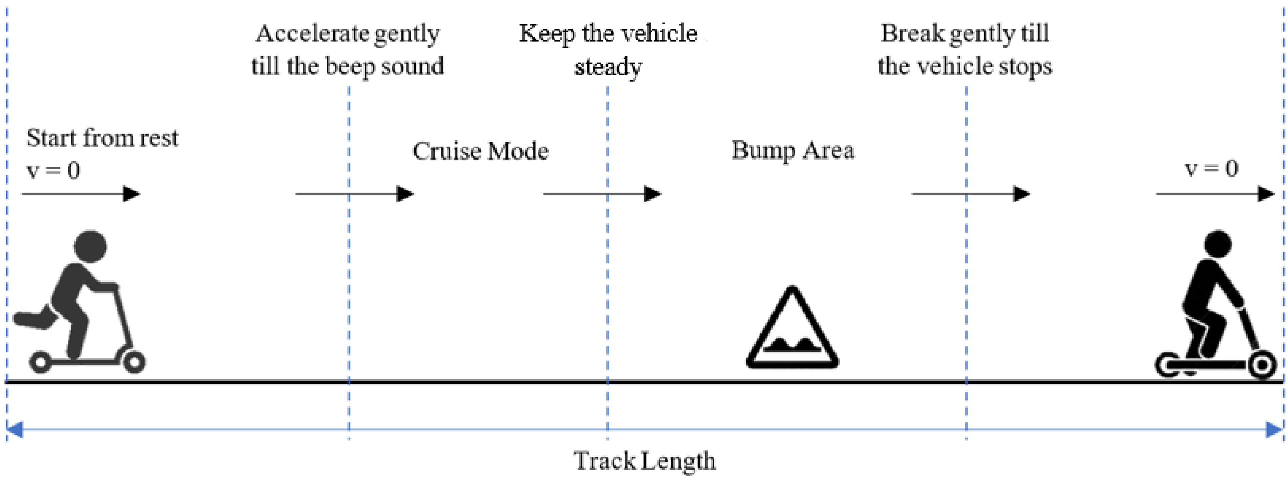

Figure 4.1.1 – Description of the task

Figure 4.1.2 – Test track

The picture above shows the test track having multiple mini-bumps with an elevation of about 2mm with a tolerance of ±0.3 mm.

4.2 Calibration

Before performing the test for vertical dynamics of the e-scooter, a calibration process was carried out to check for any discrepancies that might happen. According to the description explained in Chapter 6.1, various pre-test runs were made. Using the tablet linked with SCADAS XS, the range of vibrations were set using the “Autorange” option available. It enabled the tests to be fairly accurate by not reaching the overload limit.

Figure 4.2.1 – Calibration test-track

4.3 Evaluation

According to the preliminary analysis and with reference to Table 4.1, the parameters were set to carry out the experiments and the e-scooter was at constant velocity of 14 km/h before passing the bump area. The results acquired through various test-runs are discussed below.

4.3.1 Frequency Analysis

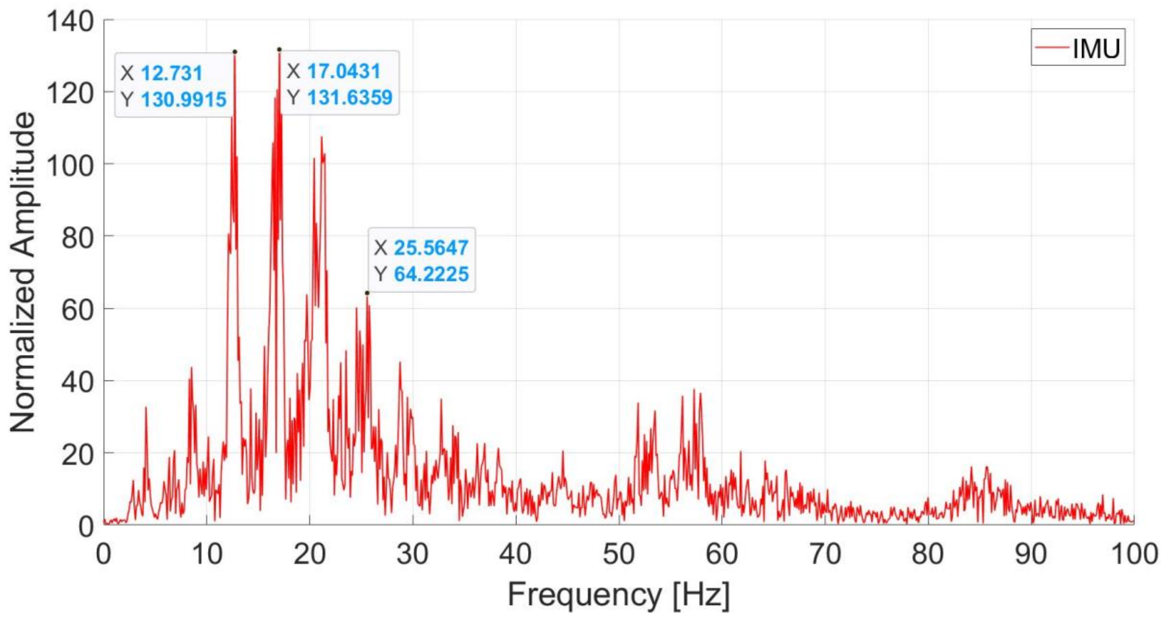

Figure 4.3.1.1 – Frequency Analysis (IMU)

Figure 4.3.1.1 and Figure 4.3.1.2 shows the signal from IMU and accelerometer respectively with respect to the vertical axis (z-axis). There is a slight difference in the amplitudes of the signal with accelerometer having greater amplitude than the IMU even though both the signals have similar peak frequencies. Therefore, the vibrations detected by accelerometer is expected to have a greater g-force than the IMU.

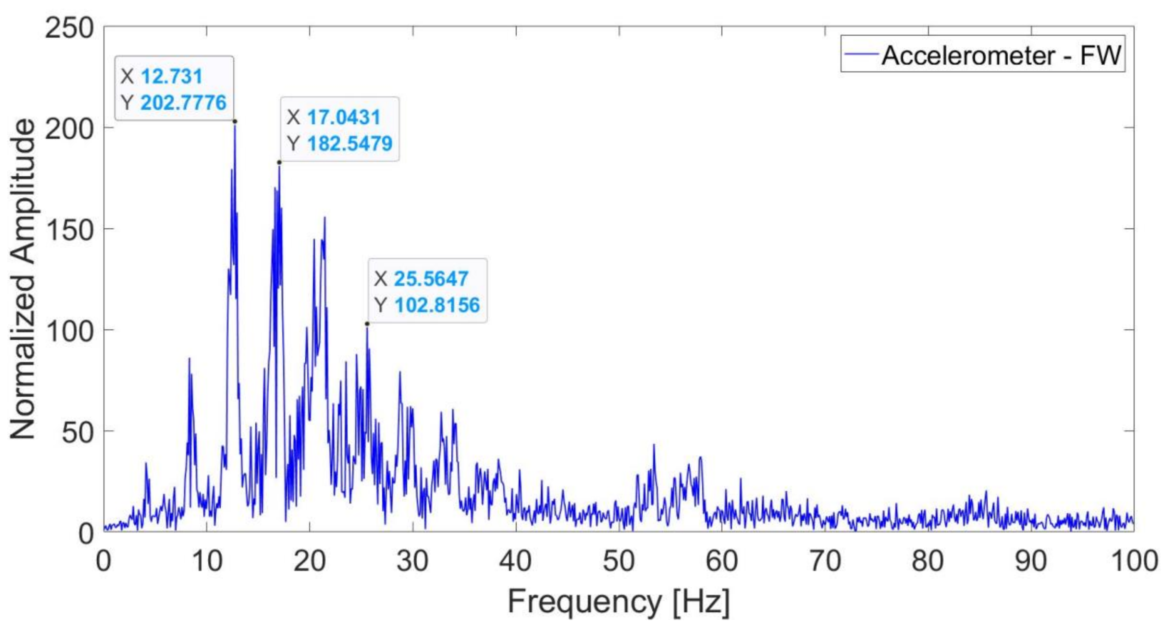

Figure 4.3.1.2 – Frequency Analysis (Accelerometer: Front Wheel)

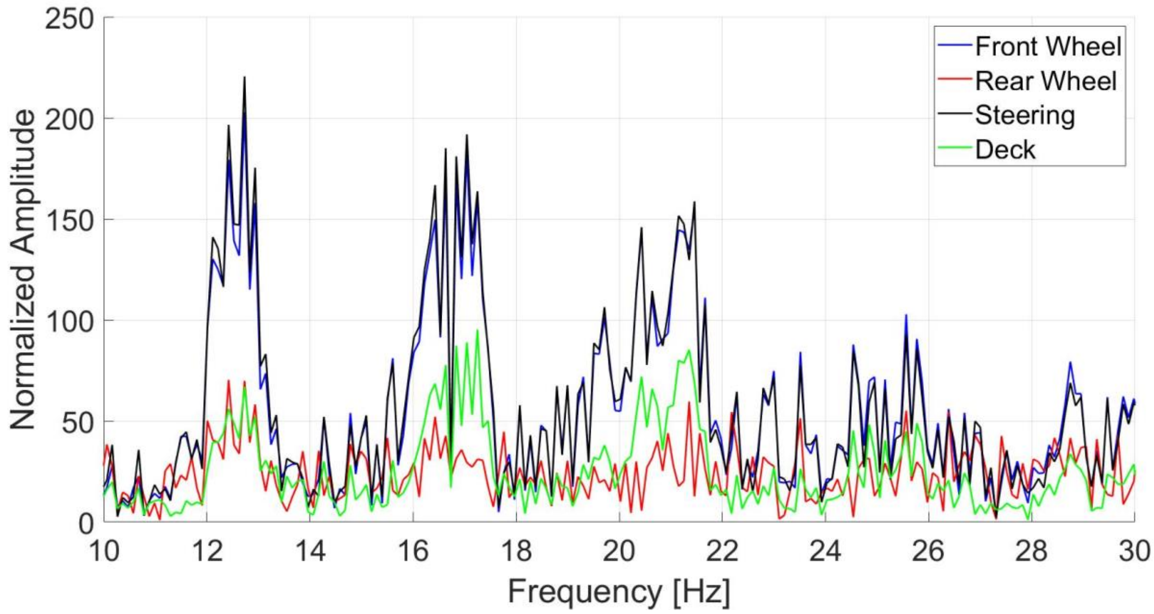

Figure 4.3.1.3 – Frequency analysis (All accelerometers)

Figure 4.3.1.3 illustrates the frequency analysis for all accelerometers. The plot is cut from the instant where the e-scooter encounters the bump. The steering column is seen to experience the highest vibration because of the peak amplitude being the greatest. The amplitude of the rear wheel accelerometer is less than the front wheel due to the fact that rear wheel has not passed the bump yet, therefore, the amplitude of rear wheel accelerometer is less.

4.3.2 Time Domain Analysis

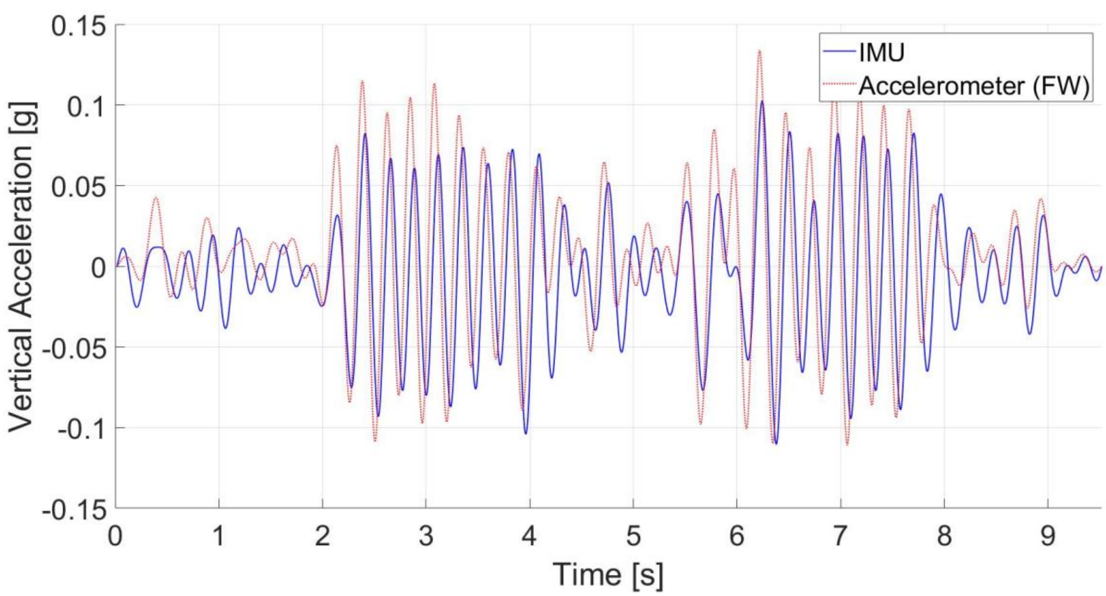

Figure 4.3.2.1 – IMU and Accelerometer (Front Wheel): z-axis

As shown in Figure 4.3.2.1, the amplitude of accelerometer is slightly greater than the amplitude of IMU as discussed in Chapter 4.3.1. This can be explained by the placement of the sensors. Figure 4.1 shows that the IMU is closer to the centre of gravity of the e-scooter and away from the front wheel as compared to the accelerometer. Therefore, the difference in amplitudes.

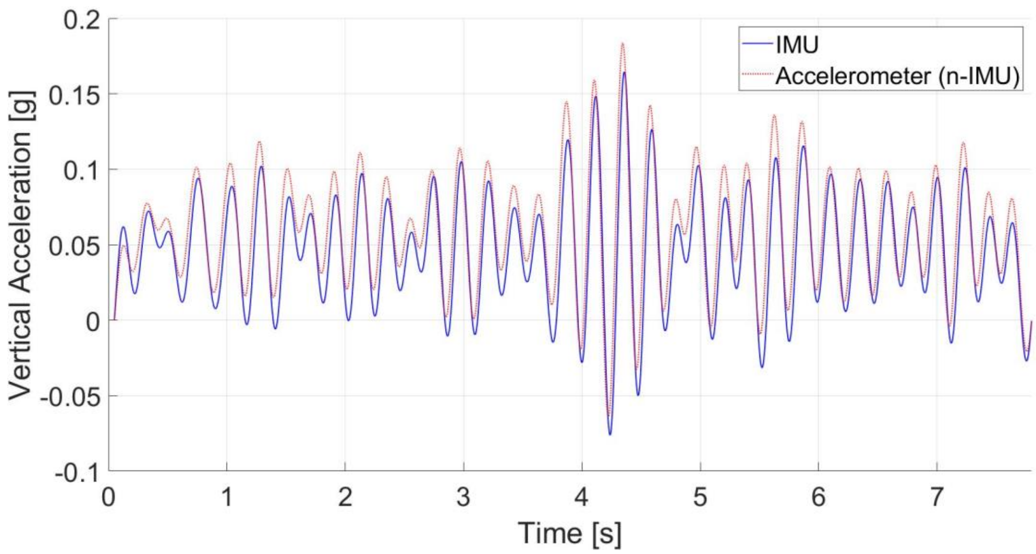

Figure 4.3.2.2 – IMU and Accelerometer (near IMU)

From Figure 4.3.2.1, we could assess that there is a difference in the amplitudes. Thus, an additional accelerometer was mounted close to the IMU for verification. As illustrated in Figure 4.3.2.2 above, the amplitudes are similar and therefore, the vibrations obtained from the IMU can be confirmed to be reliable. Similarly, another additional accelerometer was mounted close to the rear wheel accelerometer whose vibrations are depicted in the figure below.

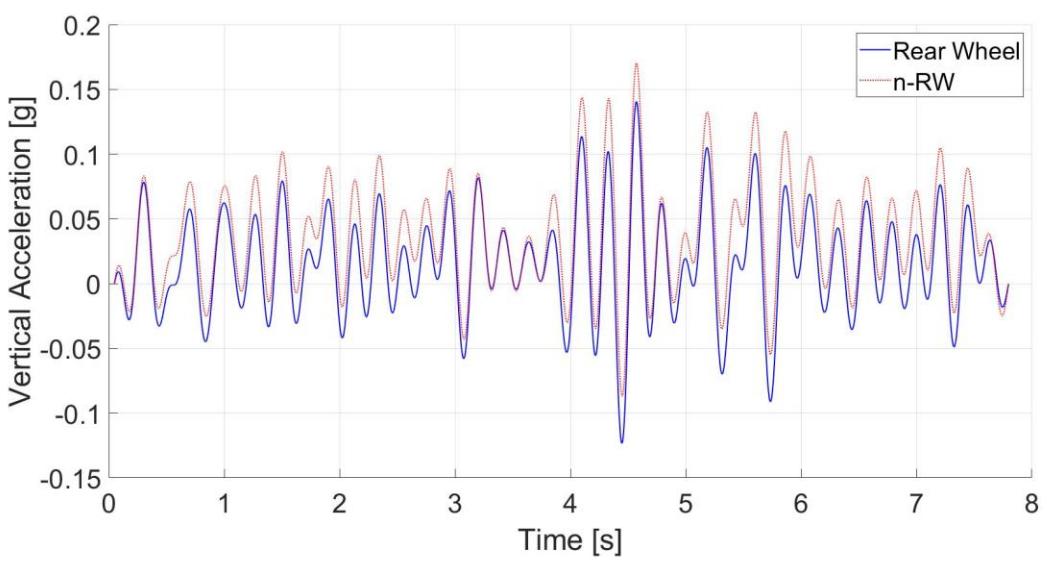

Figure 4.3.2.3 – Rear Wheel Accelerometer and Accelerometer (near Rear Wheel)

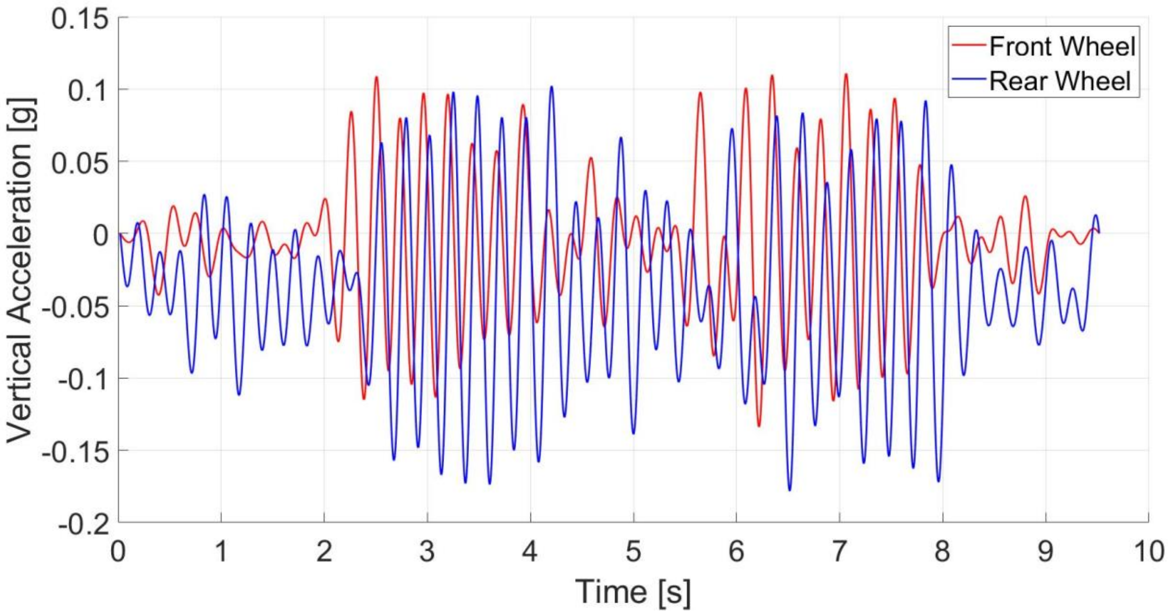

Figure 4.3.2.4 – Front and Rear

The vibrations acquired by the front and rear mounted accelerometers are illustrated in the figure above. It can be clearly understood that the vibration at the rear is more as compared to the front of the e-scooter.

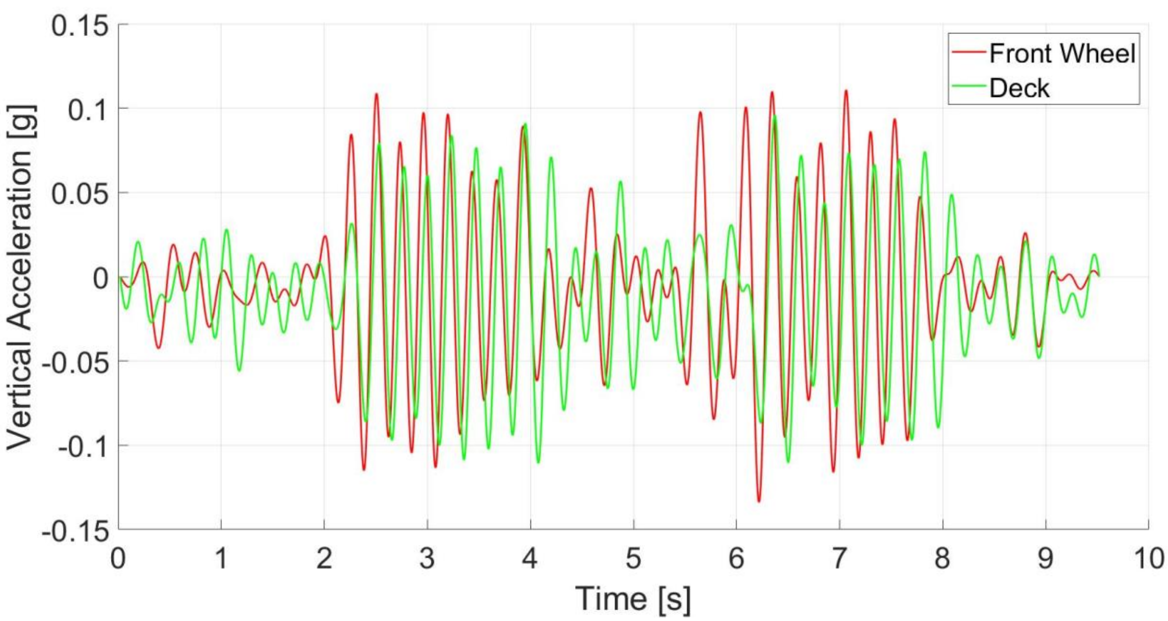

Figure 4.3.2.5 – Front and Deck

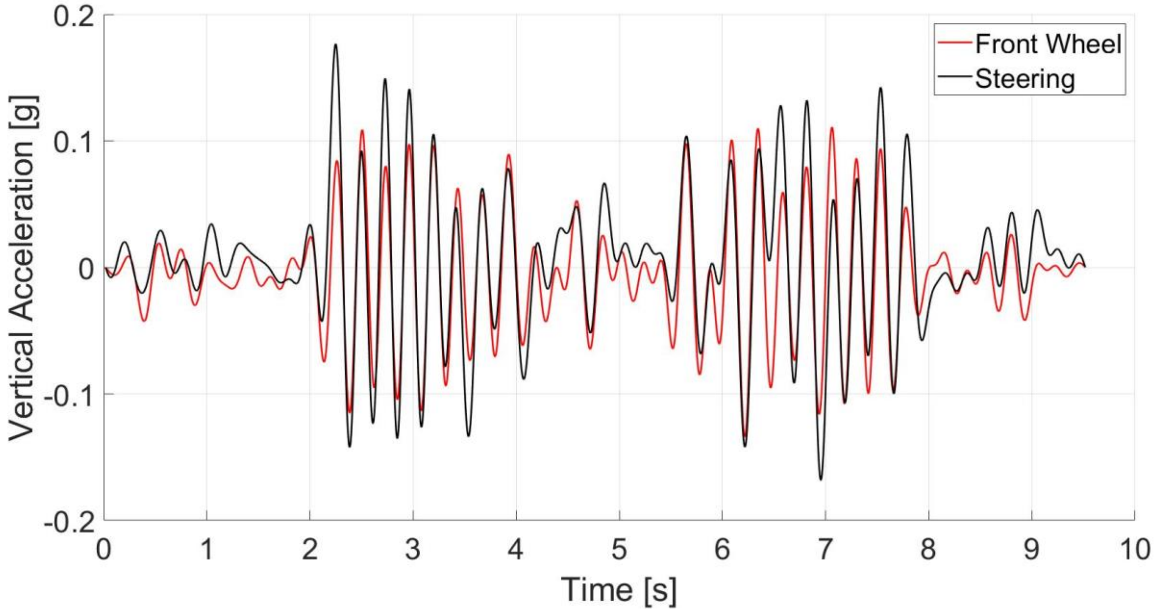

Figure 4.3.2.6 – Front and Steering

By comparing the vibration of the front accelerometer with the accelerometers mounted at the deck (platform) and the steering column as shown in Figure 4.3.2.5 and Figure 4.3.2.6 respectively, it can be inferred that steering column experiences the greatest vibration of all, but it is within the range ± 0.2g.

The individual vertical acceleration from each accelerometer is illustrated in the figure below.

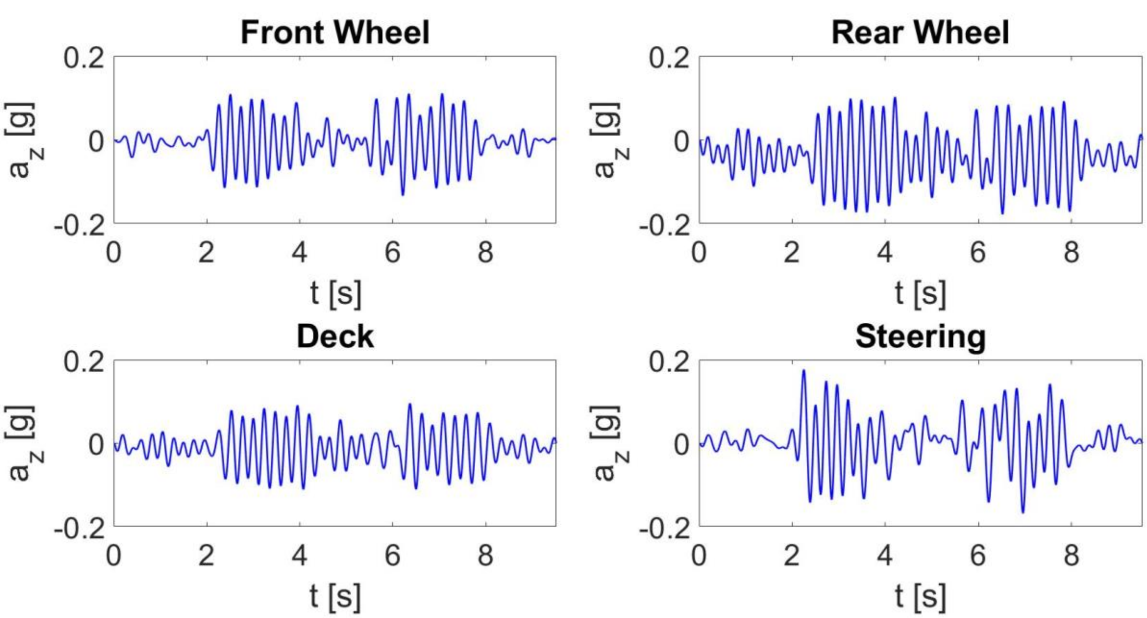

Figure 4.3.2.7 – Vertical acceleration from the Accelerometers

5. Conclusion

The e-scooter performed well in terms of maneuverability since the steering angle needed is small. The e-scooter allows two different modes, namely, driving and sport, which is distinguished by their maximum speed. The acceleration performance in both the modes are decent and the maximum acceleration was less than +0.3g. Although, the acceleration due to braking was less than -0.6g with the addition of regeneration modes in the e-scooter and can be considered safe, the braking distance processed was up to 5 m. Since, the braking performance is an important factor of safety, the e-scooter may need some development regarding the braking performance.

Also, during the vertical dynamics analysis, the e-scooter proved to be stable while passing bumps on different velocities. The vibrations on different locations of the e-scooter were assessed with a maximum vibration of ±0.2g at the steering column.

5.1 Future work

In this thesis, only an e-scooter, MI Pro 2 was studied. There are a lot of different models of these vehicles and also a lot of other electric micro-mobility vehicles that would be interesting to study. To validate the results, more data need to be collected through different participants in the analysis.
The experimental protocol also needs to do a naturalistic testing with the e-scooter to investigate the safety in a real traffic situation. An example could be for the braking behavior at a crossing where the results could be compared to the braking performance in this study.

The results can be used to help improve the design of e-scooter and contribute to guidelines for infrastructure design and policy making. The results could also be used as a baseline for future studies of different electric micro-mobility vehicles and more realistic testing.

References

[1] J.Y. Wong, *Theory of ground vehicles*, John Wiley & Sons Inc., New York, 2001.

[2] Singiresu S. Rao, *Mechanical vibrations*, Pearson Education Inc., Miami, 2011.

[3] Carsten Schedlinski, Michael Link, "A survey of current inertia parameter identification methods", *ICS Journal*, IC 63225, 2000.

[4] Zeit T. Cai, Jeremy John Worm P. E., Drew Dosson Brennan, "Experimental studies in ground vehicle coastdown testing", *ASEE Journal*, AC 2012-5030, 2012.

[5] Koken Michael, "The experimental determination of the moment of inertia of a model airplane", *Research Projects*, 585, 2017.

[6] Daniel Garcia Vallejo, Werner Schiehlen, Alfonso Garcia Agundez, "Dynamic, control and stability of motion of electric scooters", *IAVSD Journal*, 978-3-030-38077-9_139, 2020, pp.1199-1209.

[7] Paolo Baldissera, "Proposal of a coastdown model including speed dependent coefficients for the retarding forces", *Sage Journal*, ISSN 1754-3371, 2021, pp.154-163.

[8] Moad Kissai, Bruno Monsuez, Xavier Mouton, Didier Martinez, Adriana Tapus, "Importance of Vertical Dynamics for Accurate Modelling, Friction Estimation and Vehicle Motion Control", *International Automotive Congress*, Brasov, Romania, 2010.

[9] Ion Preda, Dinu Covaciu, Gheorghe Ciolan, "Coast down test theoretical and experimental approach", *21st International Conference on Intelligent Transportation Systems (ITSC)*, Maui, United States, 2018, pp.1370-1377.

[10] Rahul Ahlawat, Jurgen Bredenbeck, Tatsuo Ichige, "Estimation of road load parameters via on-road vehicle testing", A&D Europe GmbH, The Tire Technology Expo, Germany, 2013.

[11] Pavel Brabec, "Methodology for the experimental determination of the powertrain's inertia ellipsoid and its verification", MATEC Web of Conferences, 2017.

[12] Murat Ates, Ronald D. Matthews, "Coastdown coefficient analysis of heavy-duty vehicles and application to the examination of the effects of grade and other parameters on fuel consumption", SAE Paper 2012-01-2051, 2012.

[13] Mi Electric Scooter Pro User Manual, 2014.

[14] Peter Norrby, *Prediction of coastdown test results, Statistical study of environmental influences*, M.Sc Thesis, Chalmers University of Technology, Gothenburg, Sweden, 2012.

[15] Adria Bordes Roca, *Impacts of implementation of electric scooters in daily transport*, M.Sc Thesis, University of Gavle, Sweden, 2019.

[16] Lucas Billstein, Christoffer Svernlov, *Evaluating the safety and performance of electric micro-mobility vehicles*, M.Sc Thesis, Chalmers University of Technology, Gothenburg, Sweden, 2021.